

## MIT Open Access Articles

*Enhancement of rainfall and runoff upstream from irrigation location in a climate model of West Africa*

The MIT Faculty has made this article openly available. **Please share** how this access benefits you. Your story matters.

**Citation:** Im, Eun-Soon and Eltahir, Elfatih A. B. "Enhancement of Rainfall and Runoff Upstream from Irrigation Location in a Climate Model of West Africa." Water Resources Research 50, 11 (November 2014): 8651–8674 © 2014 American Geophysical Union

**As Published:** <http://dx.doi.org/10.1002/2014WR015592>

**Publisher:** American Geophysical Union

**Persistent URL:** <http://hdl.handle.net/1721.1/110306>

**Version:** Final published version: final published article, as it appeared in a journal, conference proceedings, or other formally published context

**Terms of Use:** Article is made available in accordance with the publisher's policy and may be subject to US copyright law. Please refer to the publisher's site for terms of use.





## Water Resources Research

### RESEARCH ARTICLE

10.1002/2014WR015592

#### Key Points:

- The effect of irrigation location and scheduling on rainfall distribution
- The mechanisms of local and remote impact of potential medium-scale irrigation
- Enhancement of rainfall and runoff upstream from irrigation location

#### Correspondence to:

E.-S. Im,  
eunsoon@smart.mit.edu

#### Citation:

Im, E.-S., and E. A. B. Eltahir (2014), Enhancement of rainfall and runoff upstream from irrigation location in a climate model of West Africa, *Water Resour. Res.*, 50, 8651–8674, doi:10.1002/2014WR015592.

Received 17 MAR 2014

Accepted 6 OCT 2014

Accepted article online 8 OCT 2014

Published online 11 NOV 2014

## Enhancement of rainfall and runoff upstream from irrigation location in a climate model of West Africa

Eun-Soon Im<sup>1</sup> and Elfatih A. B. Eltahir<sup>2</sup>
<sup>1</sup>Center for Environmental Sensing and Modeling, Singapore-MIT Alliance for Research and Technology, Singapore, <sup>2</sup>Ralph M. Parsons Laboratory, Massachusetts Institute of Technology, Cambridge, Massachusetts, USA

**Abstract** This study investigates the impact of potential medium-scale irrigation (about 60,000 km<sup>2</sup>) on the climate of West Africa using the MIT Regional Climate Model. We find that irrigation at this scale induces an atmospheric response similar to that of large-scale irrigation (about 400,000 km<sup>2</sup>) which was considered in our previous theoretical study. While the volume of water needed for large-scale irrigation is about 230–270 km<sup>3</sup>, the medium-scale irrigation requires about 50 km<sup>3</sup>, and the annual flow of the Niger river in the relevant section is about 70 km<sup>3</sup>. The remote response of rainfall distribution to local irrigation exhibits a significant sensitivity to the latitudinal location of irrigation. The nature of this response is such that irrigation from the Niger River around latitude 18°N induces significant increase in rainfall of order 100% in the upstream sources of the Niger River and results in significant increase in runoff of order 50%. This additional runoff can potentially be collected by the river network and delivered back toward the irrigation area. By selecting the location of irrigation carefully, the positive impacts of irrigation on rainfall distribution can be maximized. The approach of using a regional climate model to investigate the impact of location and size of irrigation schemes, explored in this study, may be the first step in incorporating land-atmosphere interactions in the design of location and size of irrigation projects. However, this theoretical approach is still in early stages of development and further research is needed before any practical application in water resources planning.

### 1. Introduction

The region of West Africa suffers from significant vulnerability to climate variability and climate change. This region is characterized by semiarid climate with a marked seasonality and a sharp north-south gradient of rainfall. Rainfall patterns are highly variable and rapid land use change is driven by population growth [Descroix *et al.*, 2009]. Rainfall variability is controlled under the influence of the West African Monsoon (WAM) system [Lebel and Ali, 2009] which is sensitive to both natural variability (e.g., sea surface temperature) [Nicholson *et al.*, 2000; Bader and Latif, 2003] and anthropogenic forcings such as aerosol and greenhouse gases [e.g., Ackerley *et al.*, 2011]. On the other hand, substantial changes in land use are mostly attributed to the human disturbance of land surface characteristics [Mahe *et al.*, 2005; Descroix *et al.*, 2009; Lebel *et al.*, 2009; Li *et al.*, 2007; Scanlon *et al.*, 2007]. In particular, the transformation of the natural landscape (e.g., natural bush) into cultivated area has been widely observed in the West African Sahel. For example, the fraction of cultivated land has increased more than five times in the 2000s relative to the 1950s in Niger, in proportion to the demographic change [Cappelaere *et al.*, 2009]. However, the region's unfavorable climate in terms of water availability constrains agricultural production [Cappelaere *et al.*, 2009]. Therefore, the traditional rain-fed agriculture, which is entirely dependent on the local rainfall, may not be the optimal way to meet the growing demand for water and food. In this regard, irrigation can play an important role by offering the opportunity to maintain sustainable and reliable crop production over the semiarid Sahelian region, which would otherwise not be feasible. Nevertheless, irrigated area as share of total cultivated area is estimated as less than 5%, for each of the four countries of the upper and middle Niger basin (Burkina Faso, Guinea, Mali and Niger) [Food and Agriculture Organization (FAO), 2010]. It reflects the fact that irrigation has not yet been developed as a major sector of agriculture in West Africa. Although there is potential for irrigation expansion, actual practice is quite limited due to geographic, hydrologic, ecologic, agronomic, and economic constraints [You *et al.*, 2010].

Irrigation projects are usually designed assuming that future local climate would remain the same as past climate. Significant body of research laid the foundation for how to carry this design process taking

hydrologic, ecological and socioeconomic factors into consideration. Although climate conditions have a dominant effect on irrigation, sensitivity and uncertainty of climate conditions are not precisely considered in the assessment of the profitability and potential for irrigation [e.g., *You et al.*, 2010; *Zwarts et al.*, 2005].

On the other hand, climate studies have been carried to quantify how irrigation may affect climate and what is the main mechanism that modulates irrigation-climate interaction. In an observational study on the impact of irrigation, *DeAngelis et al.* [2010] reported that July precipitation increased 15–30% in a broad region downwind of the Ogallala Aquifer over the Great Plains of the United States mainly around 1950, at the time when irrigation began ramping up significantly over the Ogallala. This study was based on a long-term record of station and gridded precipitation observations covering the entire 20th century. Vapor transport analysis conducted by *DeAngelis et al.* [2010] revealed that the increased evapotranspiration associated with irrigation is partly manifested in higher precipitation downwind. To investigate the time-varying impact of observed irrigation changes during the 20th century, *Puma and Cook* [2010] performed ensemble simulations using an atmosphere general circulation model forced by a time-varying data sets on irrigation water withdrawals. They presented global and regional-scale transient impacts on first-order atmospheric descriptors (e.g., temperature, precipitation, evapotranspiration) due to irrigation. They emphasized that future climate studies should account for irrigation in a changing climate condition, especially in regions with unsustainable irrigation resources.

Significant body of modeling studies has been performed to study irrigation-induced land-atmosphere interactions and their impacts on climate at various spatiotemporal scales [*Lo and Famiglietti*, 2013; *Ozdogan et al.*, 2010; *Kueppers et al.*, 2007; *Segal et al.*, 1998; *Cook et al.*, 2011; *Sorooshian et al.*, 2011, 2012; *Harding and Snyder*, 2012a, 2012b; *Marcella and Eltahir*, 2014; *Im et al.*, 2014a]. These studies conclude that irrigation might affect the climate by altering not only the surface energy partitioning but also the water cycle. However, the impact of irrigation on climate is still a topic for debate because the response of the climate to irrigation in models is quite nonlinear, depending on the location of the region of study, irrigation scheme used, and other assumptions incorporated into the model [*Sorooshian et al.*, 2012]. For example, anomalous soil moisture due to irrigation has opposing effects on rainfall over irrigated area, namely the enhancement of convection from increased low-level moisture and boundary layer energy, and the suppression of convection from irrigation-induced cooling [*Harding and Snyder*, 2012a, 2012b; *Im et al.*, 2014a]. Since these processes are simultaneous and interactive, the predictions regarding which process dominates depend on the climatological conditions at the given region. The impact of irrigation on rainfall is therefore a topic that deserves further investigations.

Due to its geographical location in a transition zone between wet and dry climates, West Africa is considered a "hot spot" for soil moisture-rainfall coupling [*Koster et al.*, 2004]. There are several studies that provide observational or modeling evidence of land-atmosphere interactions over West Africa [e.g., *Taylor*, 2010; *Knoche and Kunstmann*, 2013]. For example, *Taylor* [2010] showed that the trigger of convection and the propagation pattern downwind is positively related to the extent of wetland (e.g., Niger Inland Delta) from 24 year (1982–2005) infra-red cloud imagery data. This atmospheric response to wetland could be linked to a wetland breeze effect driven by the substantial perturbation to daytime sensible and latent heat fluxes that the wetland introduces. On the other hand, *Knoche and Kunstmann* [2013] showed that moisture evaporated from Lake Volta is partly transported and partly lifted by convective process using a regional climate model with evapotranspiration-tagging algorithm. Through this process, local vertical transport of water vapor eventually largely determine the distribution of tagged water in remote areas far away from the source of evaporation. Both studies clearly demonstrate the relevance of evaporated water for subsequent precipitation over West Africa, which is line with the work of *Eltahir and Bras* [1996] that well documented the role of precipitation recycling concept as a diagnostic tool for understanding the regional water cycle.

In contrast to the clear evidence for the need for irrigation expansion as well as strong land-atmosphere interaction, surprisingly few studies investigate the long-term response of the climate of West Africa to irrigation. In particular, *Im et al.* [2014a, hereinafter Im14] studied the impact of large-scale irrigation ( $\sim 400,000 \text{ km}^2$ ) on the WAM using a state-of-the-art MIT regional climate model MRCM [*Im et al.*, 2014b], and emphasized the dependence of the results on the location of irrigated areas. Based on the sensitivity experiments that were designed to discern the effects of irrigation location and scheduling, Im14 showed that an optimal irrigation location and scheduling exists that would lead to a more efficient use of irrigation

water i.e., increases in regional rainfall exceeds applied irrigation water significantly. Although this finding could have an important implication for many countries in West Africa, it is based on a theoretical approach that lacks the potential for practical application because of the large-scale nature of land conversion and associated water use. Large-scale irrigation is defined as an area of about 400,000 km<sup>2</sup> using irrigated water of about 100–300 km<sup>3</sup>/yr, depending on location. These assumed changes are too large for realistic development scenarios, considering that the annual flow of the Niger River basin is about 182 km<sup>3</sup> [Andersen *et al.*, 2005]. The theoretical experiments performed by Im14 have the advantage of enabling clear identification of the physical mechanisms driving the response of regional climate to irrigation prior to further more realistic simulations. In this study, we build on previous theoretical findings regarding the atmospheric response to irrigation in more practical way by investigating the impact of potential medium-scale irrigation defined as an area of about 60,000 km<sup>2</sup> in West Africa. As the irrigated area is reduced, the water needed to irrigate the target region becomes significantly less. This reduction is a very critical factor in judging the potential for irrigation development in areas where available water is limiting. Our analysis focuses on the rainfall and runoff changes in response to irrigation, and attempts to identify the optimal location and frequency of application of water.

Although this study includes numerical experiments presented within a more realistic framework than Im14 in terms of area size and water intake for irrigation, its nature is still somewhat theoretical. We do not make any specific practical proposal or conclusion based on solely the perspective emphasized in this study. The feasibility of irrigation development must take into account an integrated assessment that considers as many factors as possible across boundaries of disciplinary fields. For example, You *et al.* [2010] apply a combined approach including bio-physical and socio-economic fields to assess the potential for irrigation investment in Africa. They investigate various factors impacting production including geography of irrigated agriculture, water delivery costs, maximizing additional revenue due to irrigation. In this study we are attempting to take a step forward and bridge two areas of research: irrigation development and land-atmosphere interactions. We explore the theoretical question of how a large irrigation project in West Africa can be located and sized to achieve desirable impacts on the rainfall distribution. This may be a first step in incorporating land-atmosphere interactions in the design of location and size of irrigation project.

The specific objectives of this study are 1) to investigate optimal location and timing for water application in a medium-scale (~60,000 km<sup>2</sup>) irrigation project that maximizes the increases of rainfall and runoff upstream from irrigation location and within the Niger basin and 2) to investigate whether the physical mechanisms shaping the changes of rainfall seen in the large-scale irrigation experiments of Im14 are still valid in describing the response triggered by medium-scale irrigation, given significantly reduced forcing. If these objectives are successfully achieved, this study could provide important background to support future irrigation initiatives over this semiarid region, and then to move forward by considering practical applications such as smaller-scale irrigation, water collection methods, and the engineering design to deliver irrigation water from the Niger River to the irrigation site.

## 2. Model Description and Experimental Design

### 2.1. The MIT Regional Climate Model and Data Used

In this study, the MIT Regional Climate Model (MRCM) is used to examine the effects of medium-scale irrigation on the West African Monsoon system. Based on Regional Climate Model Version 3 (RegCM3) [Pal *et al.*, 2007], MRCM maintains much of the structure of RegCM3 but with several important improvements, including (1) coupling to the Integrated Biosphere Simulator (IBIS) land surface scheme [Winter *et al.*, 2009]; (2) a new bare-soil albedo assignment method [Marcella, 2012]; (3) new convective cloud and convective rainfall auto-conversion schemes [Gianotti and Eltahir, 2014a, 2014b]; and (4) modified boundary layer height and boundary layer cloud schemes [Gianotti, 2012]. To investigate the impact of these newly implemented or upgraded physical schemes, Im *et al.* [2014b] completed a series of experiments over the same domain of West Africa used in this study (see Figure 1a). Based on Im *et al.* [2014b], simulations of the WAM show a significant sensitivity to the choices of the land surface and convection schemes. Compared to the combinations of Biosphere-Atmosphere Transfer Scheme (BATS) land surface scheme and two convection schemes (Grell with the Fritsch-Chappell closure and standard Emanuel) that are default schemes within RegCM3, the simulation with the combination of IBIS land surface scheme and the modified Emanuel scheme shows

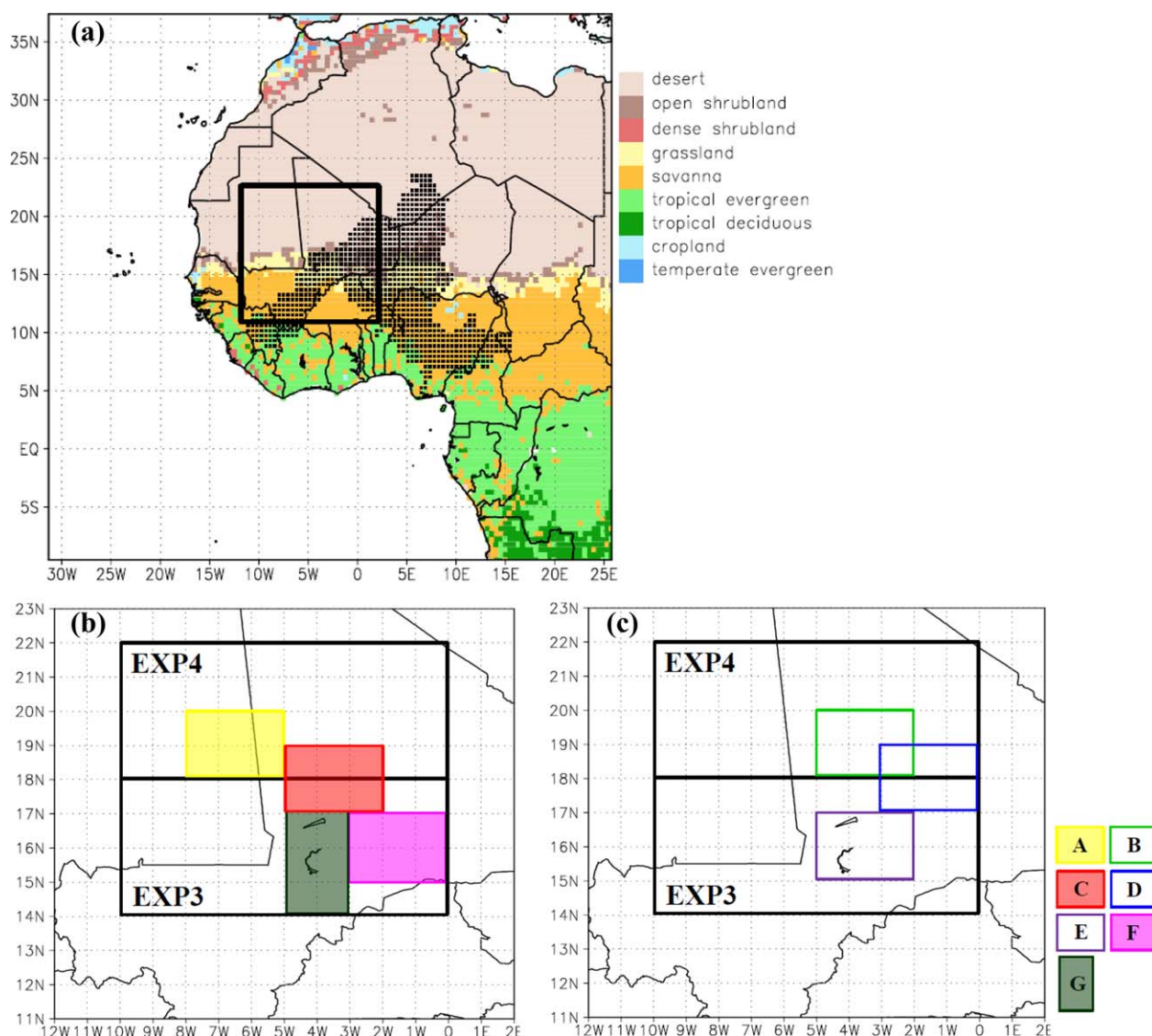


**Figure 1.** (a) Model domain and land-use distribution for the CONT and sensitivity experiments. Here superimposed dots indicate the Niger River basin. (b, c) Enlarged view of black outline in appeared Figure 1a. Two large black rectangles indicate the irrigated area for EXP3 and EXP4 seen in I14 while small colored rectangles indicate the irrigated areas for sensitivity experiments used in this study. The experiments with shaded boxes in Figure 1b, EXP3, EXP4, EXP5, and EXP6, are focused on in the analysis. Here the letters inside each rectangle correspond to the experiments denoted in Table 1.

the best performance with respect to the rainfall, surface energy balance, and the dynamics of the WAM. Therefore, we adopt the same version of MRCM for this study. More detailed model description and validation of MRCM's performance in simulating the WAM can be found in *Im et al.* [2014b].

*Marcella* [2012] and *Marcella and Eltahir* [2014] introduced a new irrigation scheme within MRCM. The main features of the irrigation scheme are described in the followings. Recalling the water balance equation for soil moisture in the irrigated area,

$$\Delta S = P - R - ET + I - D.$$

Essentially, the change in storage of the soil moisture of a layer,  $\Delta S$ , is calculated based on the amount of precipitation,  $P$ , that falls, reducing water that which runs off,  $R$ , and that drains into deeper layers,  $D$ , and reducing water that evaporates from the ground/canopy or transpires through plants,  $ET$ . Therefore, when specifying a set value for the root zone soil moisture, in terms of its relative saturation,  $s_r$  (volumetric soil moisture divided by porosity), one can use the above equation to calculate the amount of water needed,  $I$ ,



to irrigate a region and increase the soil moisture content up to any prescribed soil moisture level. This prescribed soil moisture value,  $s$ , the relative soil saturation, is as assumed to be the relative field capacity which is specified based on the observations of soil texture input data sets of IBIS. More specifically, for each time step in which irrigation is active, the fraction of actual water in the root zone is compared with the root zone relative soil saturation at field capacity. Then, the amount of water needed to bring soil moisture to the relative field capacity is added while satisfying the conservation of water mass in the column. This scheme also allows for scheduling to describe the timing of the supply of irrigated water. Through test application of this scheme to arable land in Niger River, *Marcella and Eltahir* [2014] confirm that the irrigation scheme of MRCM works properly, simulating a significant greening of irrigated area which could alter the local climate as well as the surrounding environment. Indeed, similar approaches to modeling irrigation via saturation to field capacity have been widely implemented within various climate models [e.g., *Kueppers et al.*, 2007; *Sorooshian et al.*, 2011, 2012; *Harding and Snyder*, 2012a, b]. We note that the irrigation scheme used in this study is suited for climate models representing how irrigation enhances evaporation and affects surface energy balance. The lateral routing of water through irrigation scheme is not considered explicitly, except for the fact that applied water to irrigation is compared to the observed flow to roughly assess the feasibility of the assumed scale of irrigation.

Using this scheme, Im14 performed several numerical experiments to examine the impact of potential large-scale irrigation on the West African monsoon. Basically, the experiment setup for this study (see section 2.2) is similar to that of Im14, except for different location and spatial extent of irrigated area. The initial and boundary conditions used by the MRCM are specified according to the ERAInterim reanalysis, which is the third generation ECMWF reanalysis project, with a resolution of  $1.5^\circ \times 1.5^\circ$  at 6 h interval [*Uppala et al.*, 2008]. All simulations span continuously 20 years from January 1989 to December 2008. Although additional spin-up time is not added, this should not introduce a significant error because initial soil moisture conditions are specified from long-term offline simulations that bring soil moisture in equilibrium with the climate of the region, and the analysis is focused on the summer season. The sea surface temperatures (SSTs) are prescribed by the National Oceanic and Atmospheric Administration (NOAA) Optimum Interpolation (OI) SST data set with a horizontal resolution of  $1^\circ \times 1^\circ$  and weekly resolution during the whole simulation period (1989–2008).

Simulated rainfall and runoff over the Niger River basin are evaluated against various observations. To assess the performance of the model in simulating monthly rainfall, the Climate Research Unit (CRU) Time Series 2.0 (TS2.0) [*Mitchell et al.*, 2004] and the Tropical Rainfall Measuring Mission (TRMM) 3B42 product [*Huffman et al.*, 2007] are used. In our analysis of daily rainfall, we also used TRMM 3B42 product with daily time scale. Since TRMM data are only available from 1998, an 11 year average is compared. As for the validation of runoff, monthly mean climatology provided by Global Runoff Data Center (GRDC) is used [*Fekete et al.*, 2002] (data were downloaded from <http://www.bafg.de/GRDC>). This is a global runoff field estimated by merging runoff simulations from a water balance model with observed discharge. Long-term mean runoff within the total catchment area indicates the long-term mean discharge at a gauging station divided by the total catchment area.

## 2.2. Experimental Design

Figure 1a presents the model domain and land-use map for the control experiment (CONT) without irrigation and various sensitivity experiments with irrigation. The entire domain covers most of West Africa and the Atlantic Ocean centered at  $3^\circ\text{W}$  and  $15^\circ\text{N}$  with 50 km horizontal resolution (130 grid points zonally and 114 grid points meridionally), including the whole Niger River basin. This domain is selected to simulate weather systems moving around Niger Basin without obvious interference from the boundaries. It corresponds to the typical area selected for the simulations that target West Africa [e.g., *Sylla et al.*, 2009; *Abiodun et al.*, 2012; *Marcella and Eltahir*, 2014]. The horizontal resolution of 50 km is fine enough but not ideal to fully capture the complexity of the topography and land use structure. However, the many sensitivity experiments with 20 year integration period would require a compromise between higher resolution and computational efficiency. Since we are interested not only in the local effect over irrigated area itself but also the remote effect across whole West Africa, we do not apply the nesting technique with a higher resolution over specific target area. Experiments with higher resolution (e.g., 20–25 km) will be considered for future work in order to apply much smaller-scale irrigation. The model employs 18 vertical sigma levels, from the surface to the 50 mb level. In this study, the sensitivity experiments with seven different locations

**Table 1.** Summary of the CONT and Sensitivity Experiments With Different Location and Scheduling for Irrigation<sup>a</sup>

	Irrigation Area (Lon, Lat)	Irrigation Period	Irrigated Water (km <sup>3</sup> /yr)
CONT	No Irrigation	No Irrigation	
EXPA/EXPA_S	Lon: 8°W–5°W, Lat: 18–20°N	May to Sep (MJJAS)/First week of Jun-Jul-Aug (JJA)	45/12
EXPB/EXPB_S	Lon: 5°W–2°W, Lat: 18–20°N	May to Sep (MJJAS)/First week of Jun-Jul-Aug (JJA)	46/13
EXPC/EXPC_S	Lon: 5°W–2°W, Lat: 17–19°N	May to Sep (MJJAS)/First week of Jun-Jul-Aug (JJA)	46/13
EXPD/EXPD_S	Lon: 3°W–0°, Lat: 17–19°N	May to Sep (MJJAS)/First week of Jun-Jul-Aug (JJA)	49/17
EXPE/EXPE_S	Lon: 5°W–2°W, Lat: 15–17°N	May to Sep (MJJAS)/First week of Jun-Jul-Aug (JJA)	50/20
EXPF/EXPF_S	Lon: 3°W–0°, Lat: 15–17°N	May to Sep (MJJAS)/First week of Jun-Jul-Aug (JJA)	44/16
EXPG/EXPG_S	Lon: 5°W–3°W, Lat: 14–17°N	May to Sep (MJJAS)/First week of Jun-Jul-Aug (JJA)	49/21

<sup>a</sup>Here irrigated water indicates the volume of water needed for medium-scale irrigation designed by this study.

(A to G) are performed. Irrigation locations are mostly distributed across semiarid regions and carefully selected to sample latitudinal and longitudinal positions, guided by the results of Im14.

Before describing the details of irrigation locations for individual experiments in this study, we offer a brief summary of experimental design assumed by Im14, as the current study is motivated by their results. Im14 tested the sensitivity of the climate impact of irrigation with respect to location assuming seven different locations of large-scale irrigated area, which were referred to as Experiments 1–7, (EXP<sub>n</sub>,  $n=1, \dots, 7$ ). The location of irrigation is moved in the meridional direction from the coast to the Sahara Desert (5°N–27°N) and in the zonal direction (10°W–0° and 0°–10°E). The results demonstrate location dependence, showing a larger sensitivity to latitudinal position rather than longitudinal position of the irrigated area. As the location of the irrigation area is moved from the coast northward, the regional rainfall change exhibits a significant decrease first, then increases gradually to a maximum corresponding to the location of EXP4 (18°N–22°N and 10°W–0°), shown in Figure 1, before it declines again. Therefore, in this study the medium-scale irrigation locations are positioned within two boundaries between EXP4, which is characterized as the optimal position for enhancing the increase in rainfall, and EXP3 (14°N–18°N and 10°W–0°), which exhibits less increase of regional rainfall but has the advantage in relative ease of water delivery from the river source to the irrigation field.

The first consideration in the design of the experiments in this study is to quantify the sensitivity of the impact of irrigation on regional climate to the latitudinal position of irrigation (see Table 1 and Figures 1b and 1c). Three different latitudinal bands are assigned in EXPA through EXPF, moving progressively from north to south. EXPA and EXPB are fully included within EXP4 territory, while EXPE and EXPF are located within EXP3. The extents of EXPC and EXPD lie equally within EXP3 and within EXP4. Each latitudinal band has two experiments with different longitudinal locations, thus comparing them makes it possible to elucidate the sensitivity to the longitudinal location of irrigation. In addition, the EXPG is designed to mimic the conditions in the Inland Delta of the Niger basin, which consists of braided streams, swamps, and lakes. Therefore, we simulate approximately the effect of the natural flooding over the Inland Delta that creates a large swampy area. Hence, EXPG could be interpreted as the closest to actual present conditions.

The water amount for irrigation is determined by the climatological condition (e.g., rainfall amount) and soil properties of a given location. For example, the rate of infiltration is a function of soil texture, and soil properties determine the storage capacity of soil moisture of any layer. In the case of EXPD and EXPE, the irrigated areas include a higher percent of loam rather than sand or sandy loam, so the water requirements are relatively larger than others. This is because loam texture types can hold more water, and therefore the soil moisture values at field capacity are larger [Marcella and Eltahir, 2014]. Given that in the standard experiments (EXPA to EXPG), we use irrigation to force soil moisture close to saturation at every time step from May to September, unrealistic amounts of water may be required to satisfy that constraint. Therefore, we perform additional experiments to consider the effect of scheduling. In this case, water is only applied in the first week of June, July, and August (Table 1). Scheduling works to intermittently supply irrigation water and limits water use. The difference in water requirements with and without scheduling clearly demonstrates the efficiency of scheduling in terms of water use. In fact, scheduling makes the irrigation scheme more realistic and closer to the one practiced in the agricultural sector [Sorooshian et al., 2012]. Too much application of irrigation water, such as uniformly saturating the soil during the whole irrigation period, is not necessarily required for crop production, and leads to a significant reduction in water use efficiency.

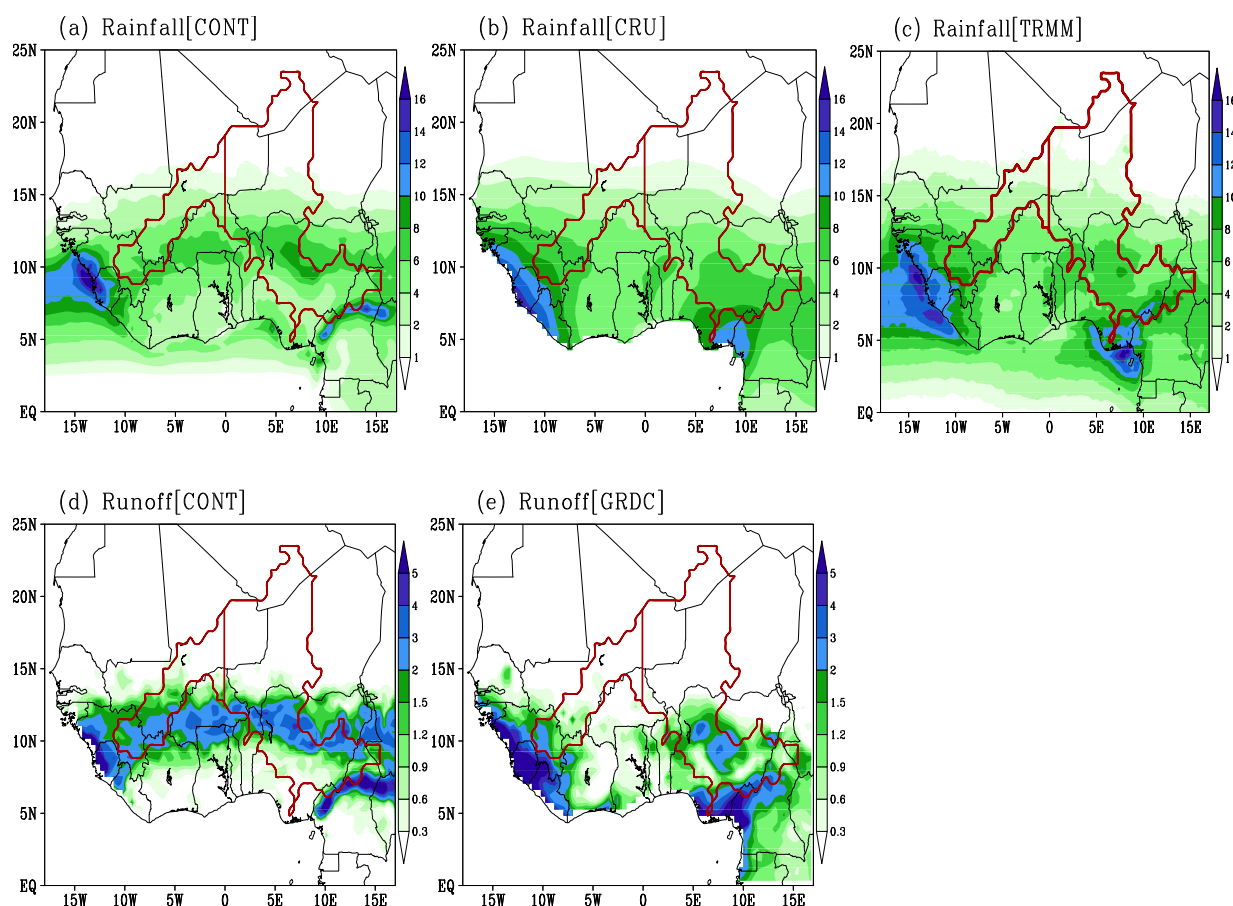


**Figure 2.** Spatial distribution of climatological (a, c) rainfall and (d, e) runoff derived from the CONT simulation and observed estimates averaged over May to September (unit:  $\text{mm d}^{-1}$ ). Here the red outline in each plot indicates the Niger River basin and its upstream subbasin (west of  $0^\circ$ ) used for area-averaged analysis.

### 3. Comparison of Simulations and Observations Over the Niger River Basin

The performance of MRCM (i.e., CONT) in simulating WAM is comprehensively evaluated against various observations in *Im et al.* [2014b]. Generally, the MRCM is capable of reproducing the main features of WAM in terms of rainfall, clouds, surface energy balance, and large-scale circulation. In particular, the spatial distribution and seasonal variation of rainfall exhibit the reasonable performance, which is comparable to various state-of-the-art regional climate models participating in the Coordinated Regional Downscaling Experiment in Africa (CORDEX-Africa) reported by *Nikulin et al.* [2012]. To keep this paper concise, we avoid duplicating the validation of all the features of WAM that appeared in *Im et al.* [2014b]. Instead, in this paper we only present the basic characteristics of rainfall and runoff focusing on the Niger River basin. The Niger River is Africa's third longest river (4200 km), and its basin has a large area (2.27 million  $\text{km}^2$ ) with significant potential for water resources development [Andersen et al., 2005; KfW Development Bank, 2010]. The diverse geographic and climatic characteristics of the Niger River basin play an important role in shaping availability of water resources, which in turn affects a range of feasible water resource-related activities (e.g., irrigation). Therefore, it is important to assess whether our modeling system is capable of adequately reproducing the observed patterns of hydrological variables over the Niger basin.

Figure 2 shows the spatial distribution of rainfall and runoff averaged for May through September (MJJAS) derived from CONT simulation and several observations. In general, the simulation results indicate a reasonable skill in capturing the main features of hydrological variables. First, the simulated rainfall shows a good agreement with observed patterns in both quantitative and qualitative aspects. For example, the model successfully reproduces the meridional gradient of rainfall with decreasing amount from the southern Sahel to northern Africa as well as the localized maxima offshore near the western coast of Guinea along  $5^\circ\text{N}$ – $10^\circ\text{N}$  and over the Cameroon Mountains. However, some deficiency of the model is apparent in the



simulated rainfall field which is underestimated in the southwestern coast of the Guinean region and the coastal region near the Cameroon Mountains. Such a bias is not limited to our model simulation, but rather seems to be a typical error documented in other regional climate simulations over West Africa [e.g., *Flaou-nas et al.*, 2010; *Sylla et al.*, 2009; *Hernandez-Diaz et al.*, 2013].

Next, the spatial distribution of runoff reflects reasonably well the hydrological regime in this region. A hydrologically active area covers the Bani and Benue Rivers, which are the main tributaries of the Niger River, while the artheic and endorheic area occupies most of the northern arid region which does not contribute to the discharge of the river itself [*Descroix et al.*, 2009]. Basically, the runoff pattern is correlated with rainfall even though their relationship is not necessarily simple due to the effect of factors such as evapotranspiration [*Fekete et al.*, 2004] and groundwater contribution to baseflow [*Mahe et al.*, 2005]. In addition, due to the water transport along the river network, the observed streamflow reflects the time delay associated with routing of the floods [*Andersen et al.*, 2005]. More specifically, the water originating from Guinea travels northeast toward the Inland Delta and is joined by water from the Bani River. The Inland Delta, in the semiarid Sahel area of Mali, is an extensive floodplain that loses a significant fraction (about 44 percent) of the inflows via seepage and evapotranspiration [*Andersen et al.*, 2005]. After passing through the Inland Delta, a reduced flow continues to flow toward the northeast until it reaches the southern flanks of the Sahara desert. Then, the river turns back by forming a great bend and changes direction southward. It eventually reaches the lower Niger River at the Gulf of Guinea after being joined by its largest tributary, the Benue River.

The hydrology of the Niger river as it reaches the Sahara desert is somewhat unique. Although the river brings significant amounts of water from the wet southern sources to the fringes of the desert, this water is not fully utilized by the people living in that region. Instead, some of the water is left to flow back from the dry region at the border of the Sahara desert to the wetter regions in the South. From the hydrologic point of view, this situation implies letting water flow from the desert region to the relatively water-rich south. This is happening in a region where farmers suffer significantly due to interannual fluctuations of rainfall amounts. This observation may serve as a motivation for irrigation development in this region.

The simulated runoff reproduces the major features of the observed spatial distribution characterized by localized maxima around the upper basin headwater and downstream over Nigeria. However, some discrepancies are also observed between simulated and observed runoff, particularly over the Inland Delta and Burkina Faso. In the model, the rainfall is the predominant input variable to derive the runoff, resulting in very similar spatial patterns between the rainfall and runoff. On the other hand, observed runoff is a result of more complicated and nonlinear interactions beyond the rainfall pattern, including nonlinearity of the runoff and evapotranspiration processes [*Fekete et al.*, 2004]. Since our modeling system does not include a realistic representation of the Inland Delta characterized by a significant reduction of runoff caused by evapotranspiration, this may translate into significant overestimation of runoff in this upstream area. Also, ignoring the transport and the delay due to flood routing through the network of channels results in a significant error in the timing of runoff compared to observations, especially over Burkina Faso.

To provide a more quantitative measure of model performance, the seasonal cycle of rainfall and runoff averaged over the entire basin and the upstream subbasin of the Niger River are compared against observations (defined as the area of the basin west of longitude 0°) (Figure 3). For rainfall, the CONT simulation reproduces the timing of the observed peak in August despite some underestimation, showing a good phase relationship with the observed rainfall. During the summer season, the simulation tends to produce higher rainfall amounts in the upstream area than in the whole basin, which is in line with observed pattern. In contrast to the rainfall pattern, the simulated runoff shows a limitation, not only in quantitative overestimation but also the timing, in particular in the upstream area. The simulation fails to capture the delay between the peaks of runoff and rainfall, due to the fact that the model does not represent the delay due to flood routing through channels. While the model tends to produce the rainfall and runoff peaks concurrently, the temporal phase of observed runoff tends to shift by 1 month later than the rainfall distribution, and thus the delayed peak appears in September. In addition to this mismatch in phase, the simulated runoff significantly overestimates observations in the upstream subbasin even though the simulated rainfall over that area underestimates observed rainfall during the peak time. Again, such discrepancies are due to the two limitations of the model: the lack of adequate representation of Inland Delta and associated swamps, and lack of any routing processes. Indeed, *Dadson et al.* [2010] showed that kinematic routing that

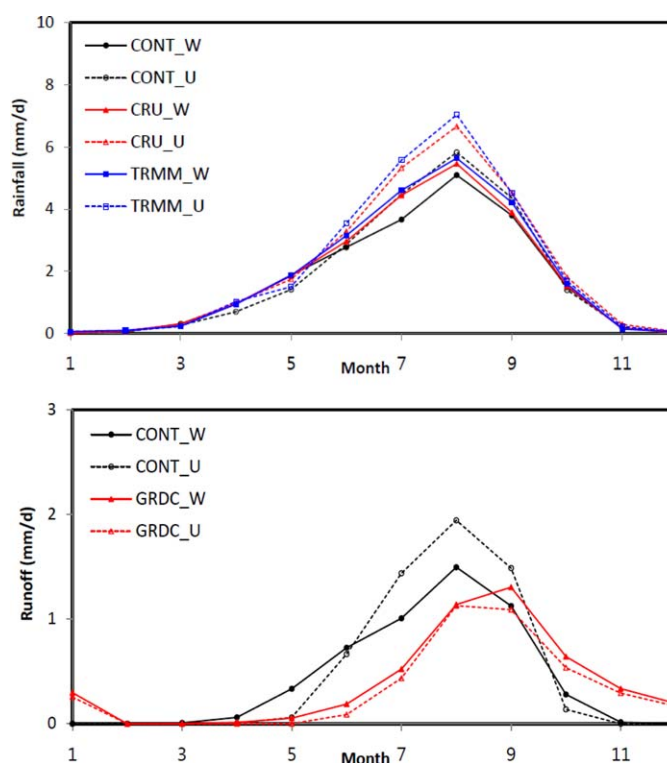


**Figure 3.** Monthly mean variation of area-averaged (top) rainfall and (bottom) runoff over the Niger River whole basin (marked "W" in the plot) and its upstream subbasin (marked "U" in the plot) derived from the CONT simulation and various observations (CRU and TRMM for rainfall and GRDC for runoff).

mean climatology for August. The presentation of mean time series gives insight into the pattern of bias in the different years. On the other hand, anomalies with respect to their respective mean climatology demon-

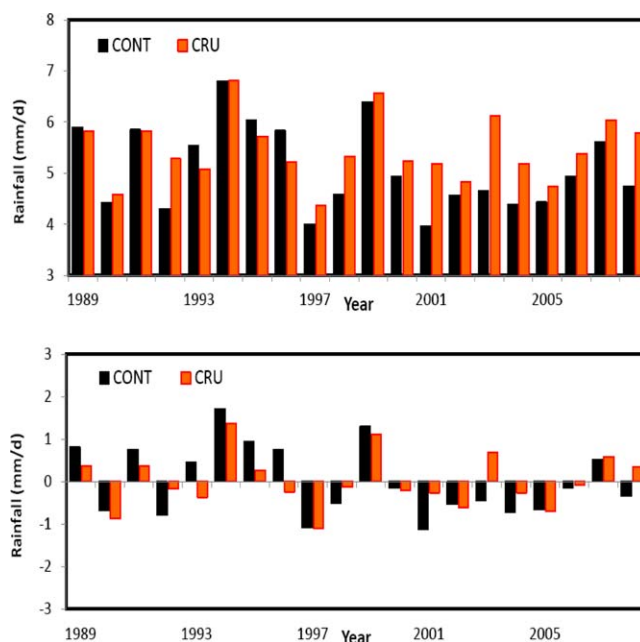


**Figure 4.** (top) Interannual variation of monthly mean rainfall in August and (bottom) its anomaly with respect to mean climatology averaged over the Niger River whole basin derived from the CONT simulation and CRU observation.

converts gridded runoff to river flow and overbank flow parameterization that considers significant evaporation loss over the Niger Inland Delta can lead to successful reproduction of time lag between peak rainfall and peak discharge in this region. Due to this reason, the problem is amplified in the upstream area including the Inland Delta particularly. Therefore, yearly mean runoff averaged over this upstream area is overestimated up to 44% (CONT\_U=176 mm/yr and GRDC\_U=122 mm/yr) while the error over the whole basin is only 8% (CONT\_W=155 mm/yr and GRDC\_W=144 mm/yr).

For more in-depth analysis of rainfall, we examine the interannual variability over the Niger basin for only August (peak time of WAM). Figure 4 shows the time series of August mean rainfall averaged over the whole basin. Figure 4 also includes the anomalies computed by subtracting

mean climatology for August. The presentation of mean time series gives insight into the pattern of bias in the different years. On the other hand, anomalies with respect to their respective mean climatology demonstrate more clearly the ability of the model to capture observed interannual variability because of the elimination of systematic bias in the underlying mean climate of the simulation. Generally, the CONT simulation shows a good agreement with observed pattern in the whole basin. The correlation coefficient in the temporal evolution of CONT simulation with CRU observation is 0.74, which is a comparable or higher value compared to other studies reported a correlation to observed summer mean rainfall over West Africa [e.g., Sylla *et al.*, 2010a, b]. The MRCM performance over the whole basin is considered reasonable.

Analysis of the monthly mean rainfall may not be sufficient to assess accurate performance of the model in simulating rainfall

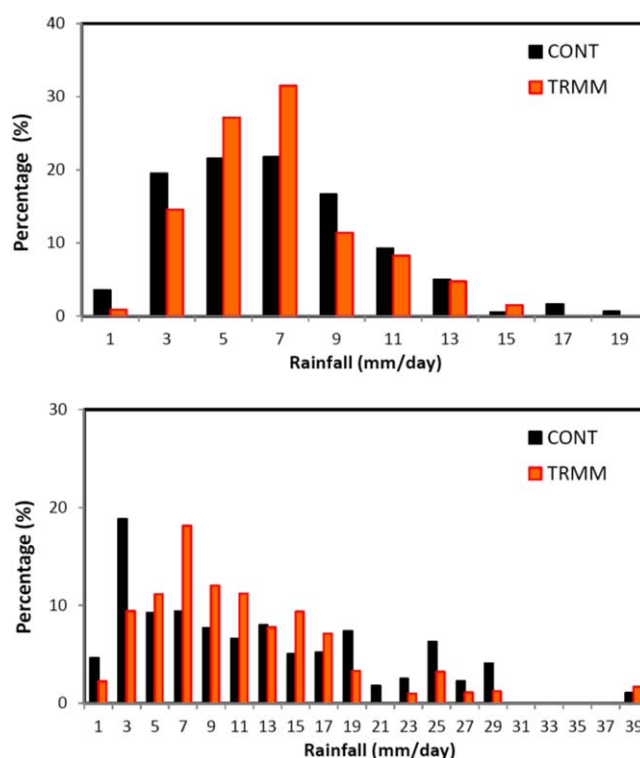


**Figure 5.** (top) Fraction distribution of the amount of rainfall as a function of daily intensity in August averaged over the Niger River whole basin and (bottom) its upstream subbasin derived from the CONT simulation and TRMM observations. Here histogram bin width is 2 mm/d and the number of x axis denotes the middle value of each bin.

in terms of the frequency and intensity of each rainfall event. Therefore, we examine the simulated daily rainfall distribution. Figure 5 shows the fraction of the simulated rainfall amount as a function of daily rainfall intensity averaged over the whole basin and its upstream subbasin. For the whole basin, the CONT simulation reasonably reproduces the general shape of distribution and the relative ratio of each intensity range. However, the model tends to underestimate high incidence observed in the intensity range of 4–8 mm/d against TRMM distribution. Consistent with the validation of seasonal cycle, the deficiency of the model becomes larger in the upstream subbasin. Underestimation for the intensities in the broad midrange and too high incidence of the first two low intensities is consistent with the negative bias of mean rainfall over the upstream subbasin. However, the CONT simulation seems to capture the tail of the intensity accurately.

## 4. Results

### 4.1. The Effect of Irrigation Location and Scheduling on Rainfall Distribution

In this section, we turn our attention to the rainfall changes in response to irrigation by comparing the simulations from the sensitivity experiments with different irrigation locations and scheduling to the CONT experiment without irrigation (see Table 1).

First, Figure 6 presents for each experiment the accumulated change in rainfall volume over the whole domain, land area, Niger River basin and its upstream subbasin relative to the supplied water for irrigation. A ratio greater than one indicates that irrigation potentially increases water availability since the water gained due to increase in rainfall is larger than the water required to irrigate, therefore this case is considered desirable and favorable in terms of water availability. Rainfall increase can occur through the mechanism of remote impact of irrigation because suppressed sensible heat flux due to cooling over irrigated area leads to the circulation change, which in turn induces an increase in moisture convergence (see the explanation of Figures 9 and 10). In addition, we carry out a two-tailed  $t$  test to examine the statistical significance of the difference between the CONT and each sensitivity experiment and the bars with black outline in Figure 6 denote that rainfall changes are statistically significant at the 95% confidence level. Furthermore, to address the consistency of the pattern of rainfall changes, we also present a fraction between zero and one that describes the fraction of simulation years with positive rainfall change due to irrigation out of a total of 20 years. Prior to looking at the detailed features of each individual experiment, this fraction considered across all experiments gives insight into the general pattern and tendency of the rainfall changes induced by irrigation location and scheduling.

This graph clearly demonstrates that irrigation has a strong impact on rainfall. The corresponding changes, their sign and magnitude, depend on the irrigation location and scheduling. Overall, there seem to be two groups: one group (EXPA, EXPB, EXPC, and EXPD, hereafter Group 1) shows a high ratio of rainfall increase to irrigation water and the other group (EXPE, EXPF, and EXPG, hereafter Group 2) shows a relatively low

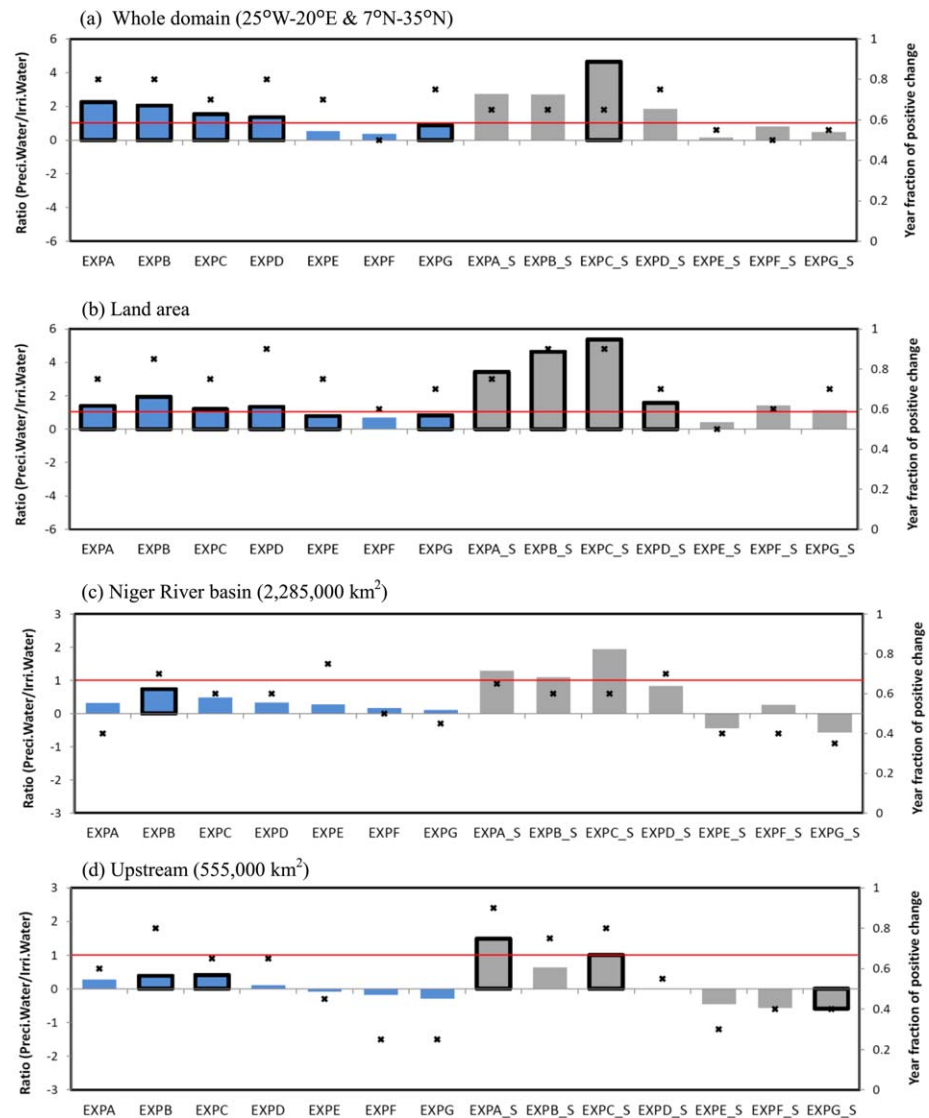


**Figure 6.** The bar indicates the ratio between accumulated rainfall volume difference (sensitivity experiment minus CONT during MJAS) over whole domain (25°W–20°E and 7°S–35°N), its land area, Niger River basin and its upstream subbasin and the amount of applied water for each irrigation sensitivity experiments. Blue and grey colors indicate the experiments without scheduling and with scheduling, respectively. Here the bar with black outline denotes statistical significance at the 95% confidence level and the cross mark indicates the fraction of year with a positive rainfall change. A horizontal red line is located at the ratio "1" that implies the same amount between the water gained due to increase in rainfall and water required to irrigate.

ratio. Such distinction becomes clearer in the scheduling experiments. The results from the two-tailed  $t$  test also support the different behavior between Group 1 and Group 2. Rainfall increases in Group 1 are more statistically significant at the 95% confidence level. In addition, the fraction of years with rainfall increase is generally higher in Group 1 than in Group 2. Thus, the rainfall increase seen in Group 1 is not a random feature of a specific year, but rather a consistent pattern in different years. In the case of Group 2, a negative ratio becomes relevant over the upstream subbasin of the Niger basin because it includes an irrigated area within that subbasin. Due to the local effect of irrigation reported by Im14, a rainfall decrease occurs over the irrigated area (see the explanation of Figures 7 and 8).

The main criterion to divide the experiments into two groups is the latitudinal location. In the experiments of Group 1 irrigation areas are located above 17°N while in experiments of Group 2 the irrigated areas are located below 17°N. Compared to the different behavior between Group 1 and Group 2, longitudinal displacement of the irrigated area seems to be less important as indicated by the relative similarity of the results of EXPA and EXPB, or EXPE and EXPF. Therefore, it is reasonable to conclude that the sensitivity of

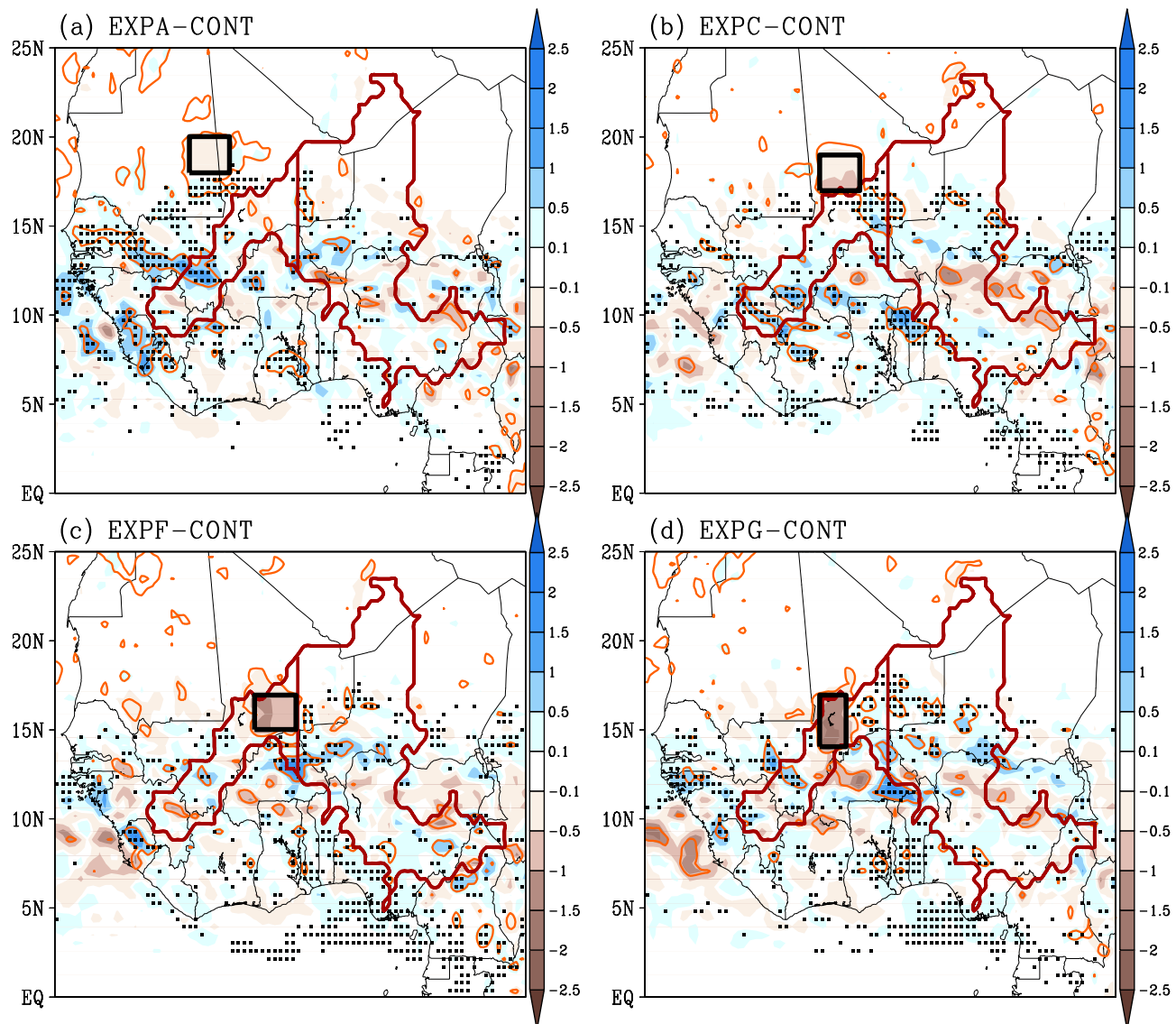


**Figure 7.** Spatial distribution of rainfall difference between irrigation sensitivity (EXPA, EXPC, EXPF, and EXPG) and CONT experiments averaged over May to September (Unit: mm/d). Superimposed dots indicate the areas where the fraction of simulated the years with rainfall increase is more than 0.6 (e.g., 13 years out of a total of 20 years). Areas enclosed by orange color line indicate the areas where the rainfall difference is statistically significant at the 90% confidence level. The region where the CONT rainfall averaged over May to September is less than 50mm is masked out of this figure. Here the black line rectangle indicates the irrigated area for each sensitivity experiment and the red outline indicates the Niger River basin and its upstream subbasin (west of 0°) used for area-averaged analysis.

rainfall change is more dependent on the latitude of irrigation location than longitude, which is in line with the results from large-scale irrigation experiments presented by Im14.

The reason that scheduling experiments, particularly with Group 1, show a much higher ratio is the reduction in the water supplied for irrigation, not any enhancement of the rainfall. As evident in Table 1, once scheduling is applied, generally less than one third of irrigation water is required. Therefore, the ratio of rainfall increase to irrigation water is significantly higher even though the rainfall increase is similar or even less compared to that from the experiment without scheduling. This means that the additional water used for irrigation is not compensated enough by increases in rainfall.

Next, we focus on the four experiments, namely EXPA, EXPC, and EXPF representing each latitudinal band and EXPG representing the Inland Delta (See section 2.2). For the sake of simplicity, we do not present the details of all experiments because EXPA (C, E) and EXPB (D, F) show generally similar patterns of change due to lack of sensitivity to longitudinal displacement. Figure 7 presents the spatial distribution of MJAS



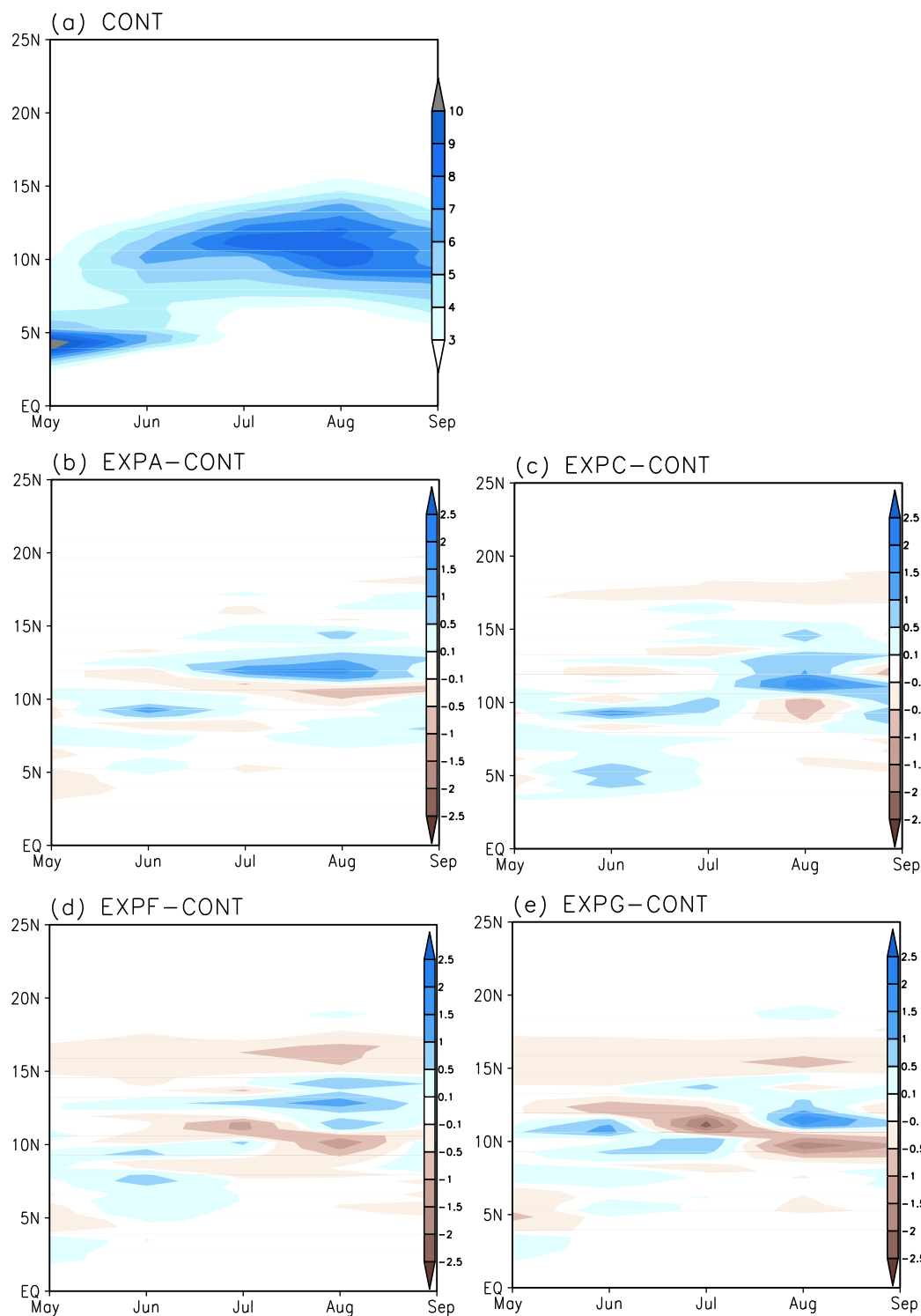


**Figure 8.** Latitude-time cross section of monthly mean rainfall averaged over 10°W–0° from (a) CONT simulation and (b–e) their difference with EXPA, EXPC, EXPF, and EXPG.

mean rainfall difference between the four sensitivity experiments and the CONT experiment. The patterns of rainfall change exhibit both increasing and decreasing signs. Though this pattern may initially seem to be chaotic, well-defined and persistent patterns can be derived from this complexity. The most consistent pattern appearing in all experiments is a decrease in rainfall over the irrigated area. The magnitude of the rainfall decrease seems to be proportional to the rainfall climatology at a given region. EXPA and EXPC with

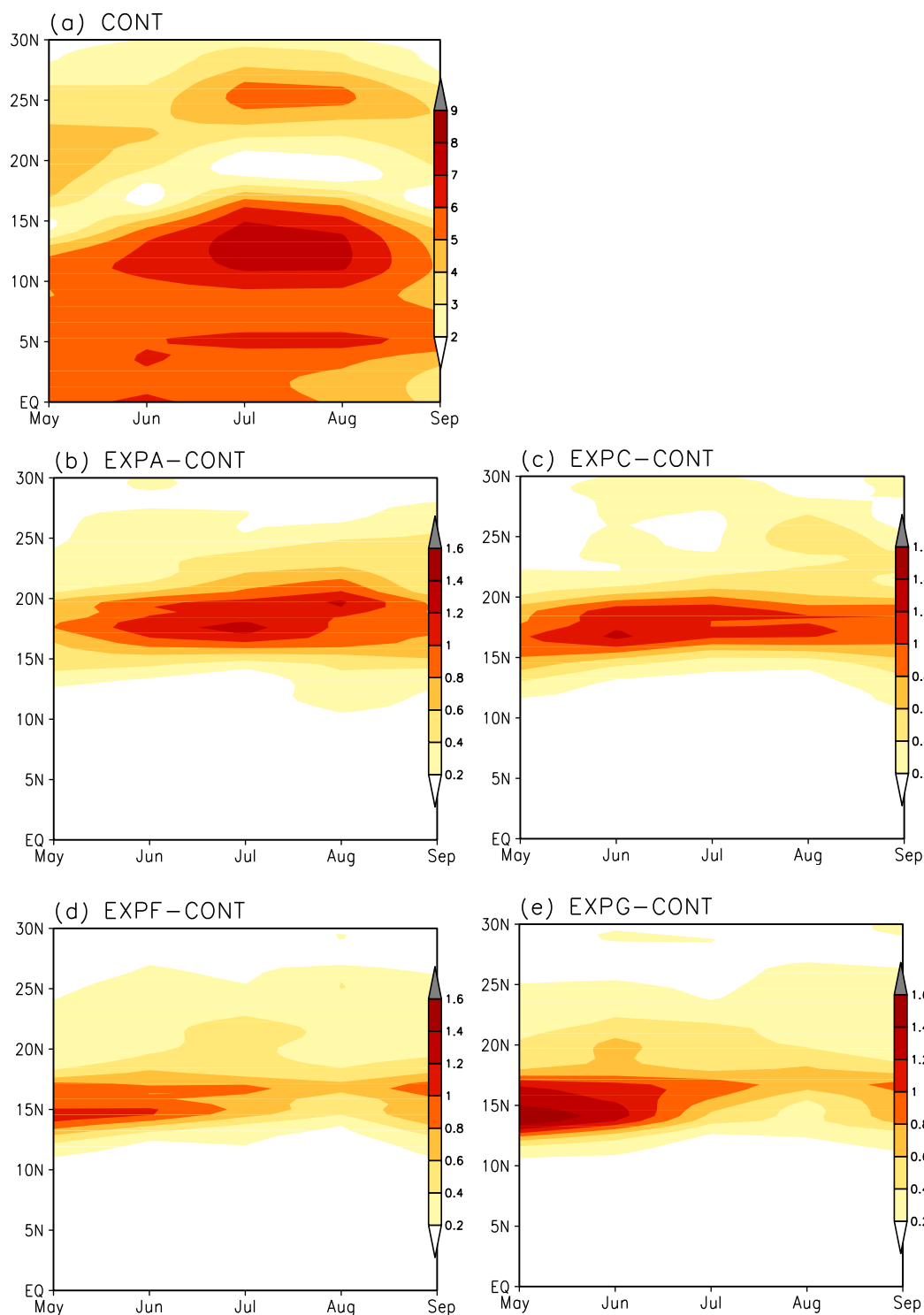


**Figure 9.** As in Figure 8 but for wind magnitude.

the irrigated areas in the relatively dry northern region show less decrease in rainfall, compared to EXPF and EXPG with the irrigated areas located in the wet southern region. Such a local change over the irrigated area is similar to the behavior presented in the large-scale irrigation experiment of Im14. Therefore, the medium-scale irrigation seems to draw the same response as large-scale irrigation, despite much reduced forcing of irrigation water. The mechanism to regulate such a local effect is proposed by Im14. Strong

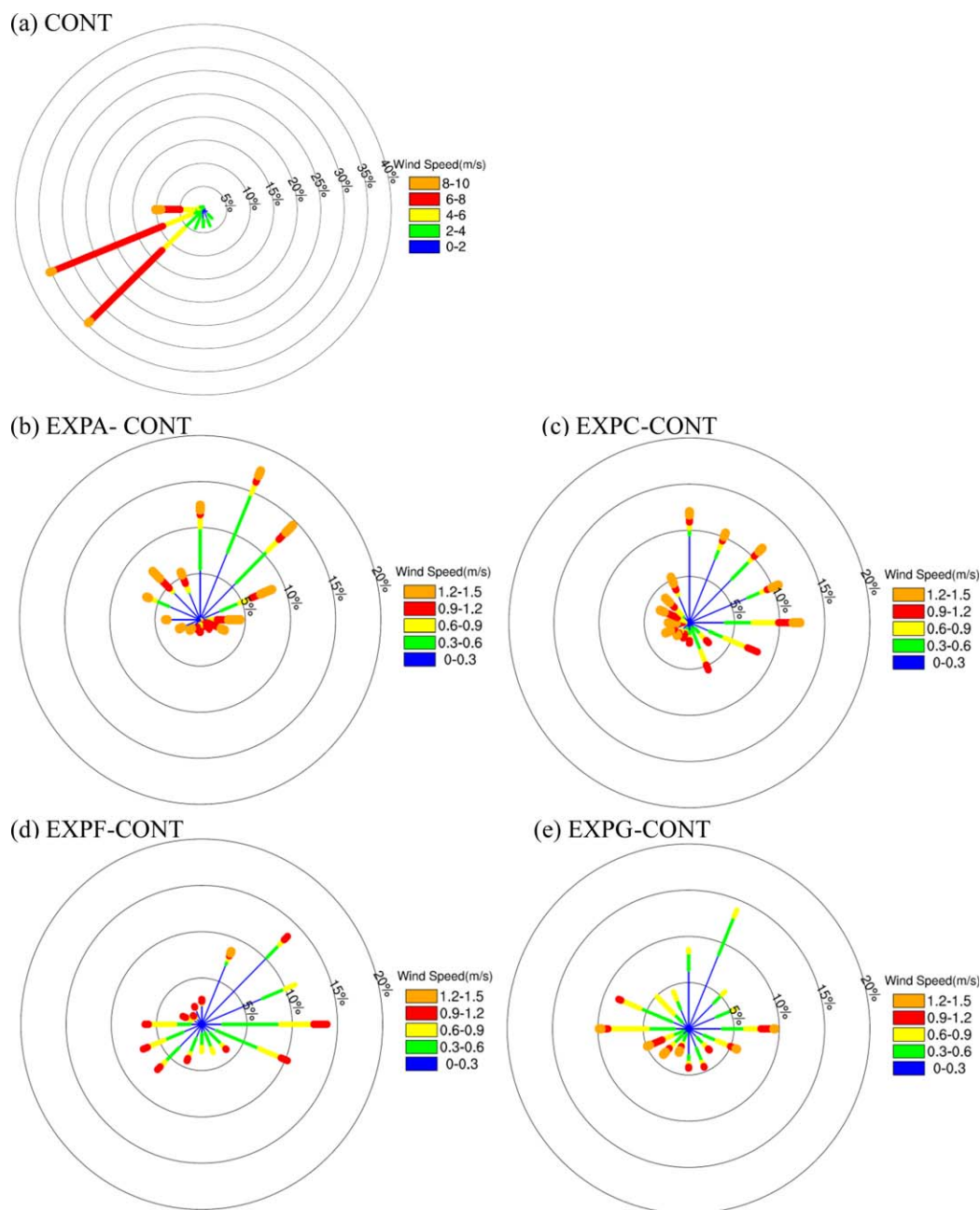


**Figure 10.** Windrose of monthly wind at 925 hPa derived from CONT simulation and its difference with EXPA, EXPC, EXPF, and EXPG ( $10^{\circ}$ – $20^{\circ}$ N and  $10^{\circ}$ W– $0^{\circ}$ ) for July and August.

surface cooling due to enhanced evaporation tends to suppress planetary boundary layer (PBL) height, which leads to inhibiting convective triggering. In spite of higher moist static energy and convective available potential energy (CAPE) owing to the increase of the total flux of heat from the wet soil [Eltahir, 1998], the frequency of convective triggering is reduced due to enhanced convective inhibition (Im14). This effect is independent of the location of the irrigated area. In contrast to the similar local response over the irrigated areas across all experiments, different behaviors between Group 1 and Group 2 become manifested at the upstream subbasin of the Niger basin. EXPF and EXPG show limited extent and magnitude of the rainfall increase in the upstream subbasin while rainfall increase is dominant in EXPA and EXPC. To address the consistency of the pattern of rainfall change at individual grid points across the different years, Figure 7 includes the information of fraction of simulation years with rainfall increase. The areas where the fraction of the simulation years with rainfall increase is more than 0.6 (i.e., 13 years out of a total of 20 years) are

overlaid by dots. We also perform the student's  $t$  test and display the areas where the rainfall changes are statistically significant at the 90% confidence level in order to diagnose the statistical significance of the rainfall changes. Note that the region where the CONT rainfall averaged over May to September is less than 50 mm is masked out of this figure to avoid the potential inflation due to small rainfall amounts. The dots coverage over the majority of blue color regions reveals that rainfall increase is probably not a random feature of specific year, but a rather consistent pattern in different years. From a statistical point of view, the statistical significance of rainfall increase due to irrigation is restricted to only small areas. However, it does not necessarily mean that rainfall increases over statistically nonsignificant areas are not meaningful. For example, some areas overlaid by dots are not significant at the 90% confidence level, but these areas indicate that the simulation year with the rainfall increase is more than 13 years out of a total of 20 years.

The response of rainfall distribution to irrigation is more clearly revealed in the meridional distribution of zonally averaged ( $10^{\circ}\text{W}$ – $0^{\circ}$ ) rainfall from May to September (Figure 8). Rainfall pattern from CONT simulation describes the climatological characteristics of the northward propagation of WAM, reaching its peak in August across the Sahel region. Consistent with mean climatology, strong responses occur mostly along the maximum band of monsoon rainfall. In line with spatial distribution, both EXPA and EXPC show a domain-wide increasing pattern of rainfall, but the areas where rainfall decreases appear rather random and with weak magnitude. By contrast, EXPF and EXPG show more intense and wide-spreading areas of rainfall decrease in addition to the decreasing band located in the irrigated area. It is important to note that the change in pattern from (EXPA and EXPC) to (EXPF and EXPG) are very similar to those from EXP4 to EXP3, presented in Im14. Based on the analysis of Im14, the main cause for the different behaviors between EXP4 and EXP3 are explained by the latitudinal location of irrigation-induced low-level flows. The position and intensity of these flows vary according to the location of irrigated area.

To examine whether the physical mechanism behind remote rainfall changes in response to large-scale irrigation found in Im14 is still valid for medium-scale irrigation, the same analysis as Im14 is performed here. Figure 9 presents the meridional distribution of zonally averaged ( $10^{\circ}\text{W}$ – $0^{\circ}$ ) wind magnitude from May to September. First of all, the climatological aspect of wind magnitude from CONT simulation is well correlated with rainfall climatology (Figure 8a). In fact, the maximum band of wind magnitude along  $10^{\circ}$ – $15^{\circ}\text{N}$  corresponds to the prevailing southwesterly monsoon flows that transport moist air from the Atlantic ocean (see the explanation of Figure 10). Therefore, the changes of wind and resultant circulation can be strong enough to change the rainfall distribution. While irrigation brings the rainfall decrease over irrigated area due to local effects, the changes over the regions far from irrigated fields are the results of a remote response to irrigation. The key for explaining the remote impact is related to modification of the WAM circulation. A rainfall decrease over the irrigated area generates anomalous descending motion, and subsequently low-level anticyclonic circulation (the same mechanism shown as Figure 8 in Im14). Since the anomalous low-level outflows blowing from anticyclonic circulation associate with the distribution of the areas with low-level convergence through interaction with the prevailing monsoon flow, the position and timing of this flow in the control climate play an important role in remotely modulating the rainfall in terms of sign and magnitude of changes. For example, the maximum outflows magnitude in EXPA and EXPC occurs after June and is located at a zone with a sharp gradient of climatological wind, and hence can be effective in producing additional convergence. On the other hand, the peak timing of anomalous wind from EXPF and EXPG simulations appears to be too early and its location is too much to the south for it to create a significant convergence with the prevailing monsoon flow. In addition to latitudinal variation of zonally averaged wind magnitude, A windrose diagram that presents how wind speed and direction are typically distributed can give further information to more clearly explain aforementioned difference between EXPA (or EXPC) and EXPF (or EXPG). Figure 10 displays the windrose plots of monthly wind at 925hPa derived from CONT simulation and its difference with EXPA, EXPC, EXPF, and EXPG during WAM peak period (July–August, see Figures 8a and 9a). Mean and anomalous wind data are collected across latitudinal range of  $10^{\circ}$ – $20^{\circ}\text{N}$  where large anomalous flows appear in Figure 9 (in the same longitudinal zone of  $10^{\circ}\text{W}$ – $0^{\circ}$ ). Climatological feature of low-level wind is characterized by predominant southwesterly flow. This is the prevailing monsoon flow over the Guinean coast and Soudano-Sahelian region, which brings moisture influx to West Africa from the Atlantic Ocean [Im *et al.*, 2014b]. Over this background climatological condition, different irrigated areas impose anomalous flows with different direction and speed as presented in Figures 10b–10e. EXPA and EXPC show low-level northeasterly which collide with the prevailing monsoon flows (southwesterly), and contribute to effectively enhance the low-level convergence. However, EXPF and

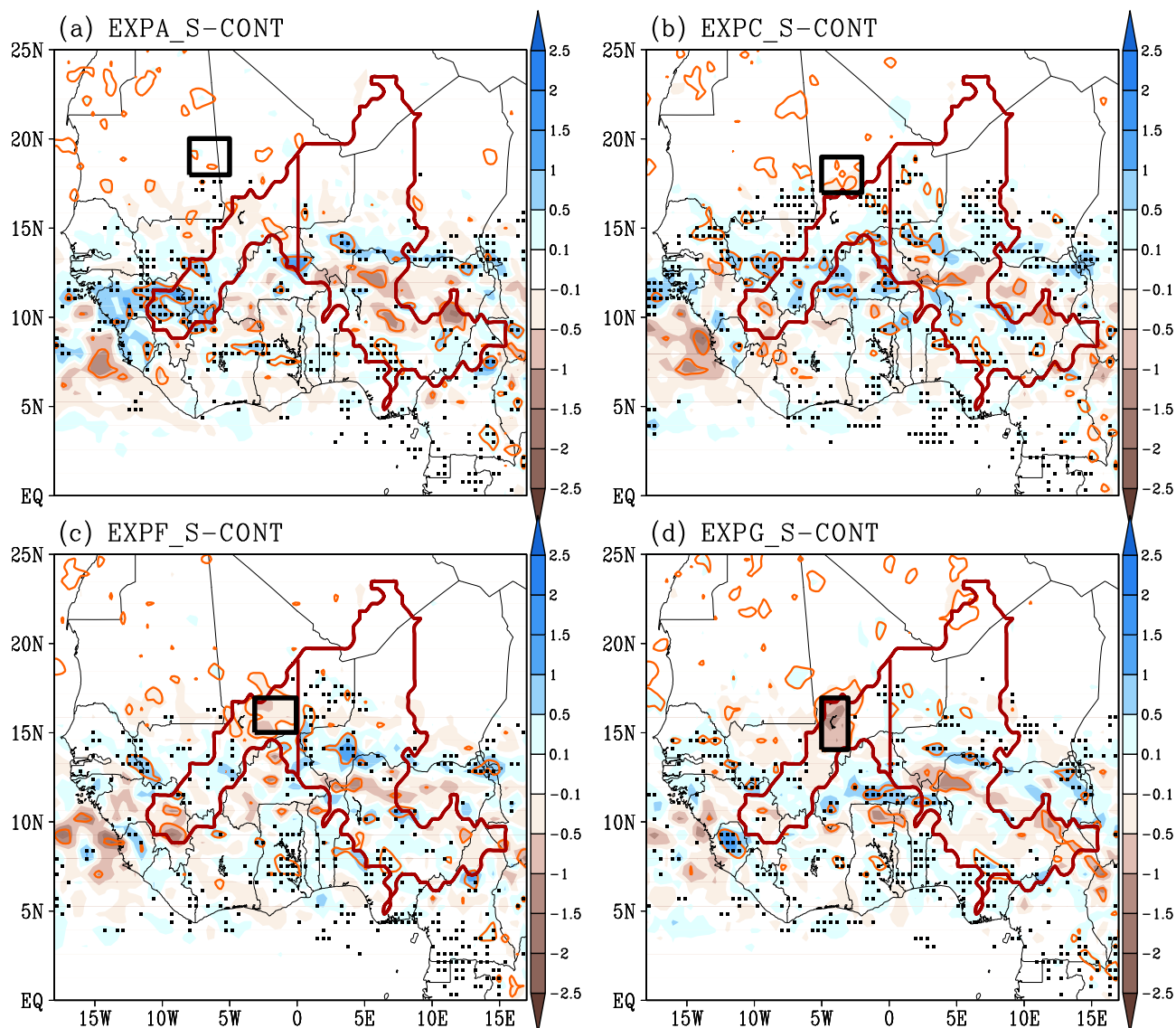


**Figure 11.** As in Fig. 7 but for EXPA\_S, EXPC\_S, EXPF\_S, and EXPG\_S scheduling experiments applied water in the first week of June, July, and August.

EXPG produce less systematic and rather diverse directions of outflows during WAM peak period. This is consistent with the results of Im14 (see Figures 11 and 12 in Im14), again emphasizing the role of optimal location and timing of induced anomalous flows for the convergence with the existing monsoon flows. Therefore, we conclude that the theory and physical mechanisms that explain the changes of remote rainfall seen in the large-scale irrigation experiments (See Im14) can be used to describe the response triggered by the medium-scale irrigation, despite the significantly reduced forcing of irrigation water.

Moving to the scheduling experiments, we can draw similar conclusions to the experiments without scheduling. Figures 11 and 12 present the rainfall change derived from the scheduling experiments in the same format as in Figures 7 and 8. Interestingly, the rainfall changes are indeed comparable to those from the experiments without scheduling, even though irrigation with scheduling consumes significantly reduced amounts of water (Table 1), which in turn induces much smaller magnitudes of anomalous wind (Figure 13). This means that an additional supply of irrigation water does not necessarily result in a proportional increase in rainfall. More importantly, this result supports the robustness of the response to irrigation in our modeling system. Based on these results and the results presented in our earlier paper (Im14), the model behavior in responding to irrigation forcing (e.g., the amount of irrigation water) is quite consistent and systematic.



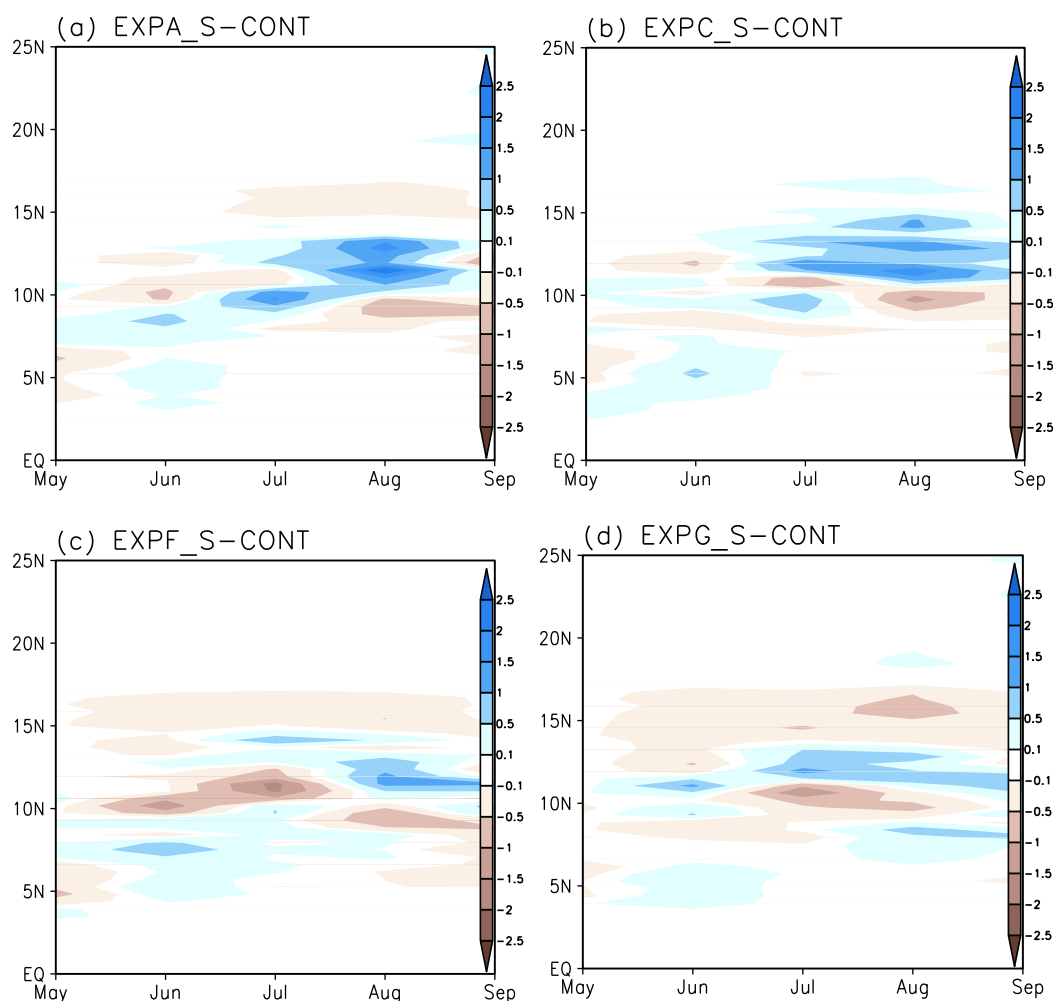


**Figure 12.** Latitude-time cross section of monthly mean rainfall averaged over  $10^{\circ}\text{W}$ – $0^{\circ}$  from the difference between EXPA\_S, EXPC\_S, EXPF\_S, and EXPG\_S and CONT simulation.

Therefore, the increase in rainfall derived from the experiment without scheduling is not caused by an exaggerated response of atmosphere due to the addition of a large mass of irrigation water into the atmosphere. The response of the atmospheric dynamics to the localized cooling is the key to explaining our results.

Basically, our model irrespective of scheduling, simulates the same patterns of the dependence of the response of rainfall to irrigation on the latitudinal location of irrigated area. Compared to EXPF\_S and EXPG\_S, rainfall increases from EXPA\_S and EXPC\_S are significantly more pronounced. Furthermore, EXPA\_S and EXPC\_S show enhanced extent and magnitude in rainfall increase during August (peak time of WAM over the Sahel region) relative to the corresponding experiments without scheduling (Figure 8 versus Figure 12).

One possible reason that scheduling experiments still produce rainfall changes equivalent to those in the experiments without scheduling can be found in the anomalous wind pattern simulated in these experiments (Figure 13). By comparison, peak positions from all scheduling experiments tend to shift 1 month later than their corresponding experiments without scheduling, leading to closer match with the maximum phase of monsoon flow. Therefore, such increased synchrony in timing between the anomalous flow and the prevailing monsoon flow allows for a more effective interaction, despite significantly reduced magnitude.

#### 4.2. Enhancement of Rainfall and Runoff Upstream From Irrigation Location

The potential enhancement of rainfall and runoff upstream from the location of irrigation can be of significant practical value. The issue of rainfall upstream changes is only important as they relate to runoff changes. Under the increased conditions of rainfall upstream, the upstream catchment of the Niger River

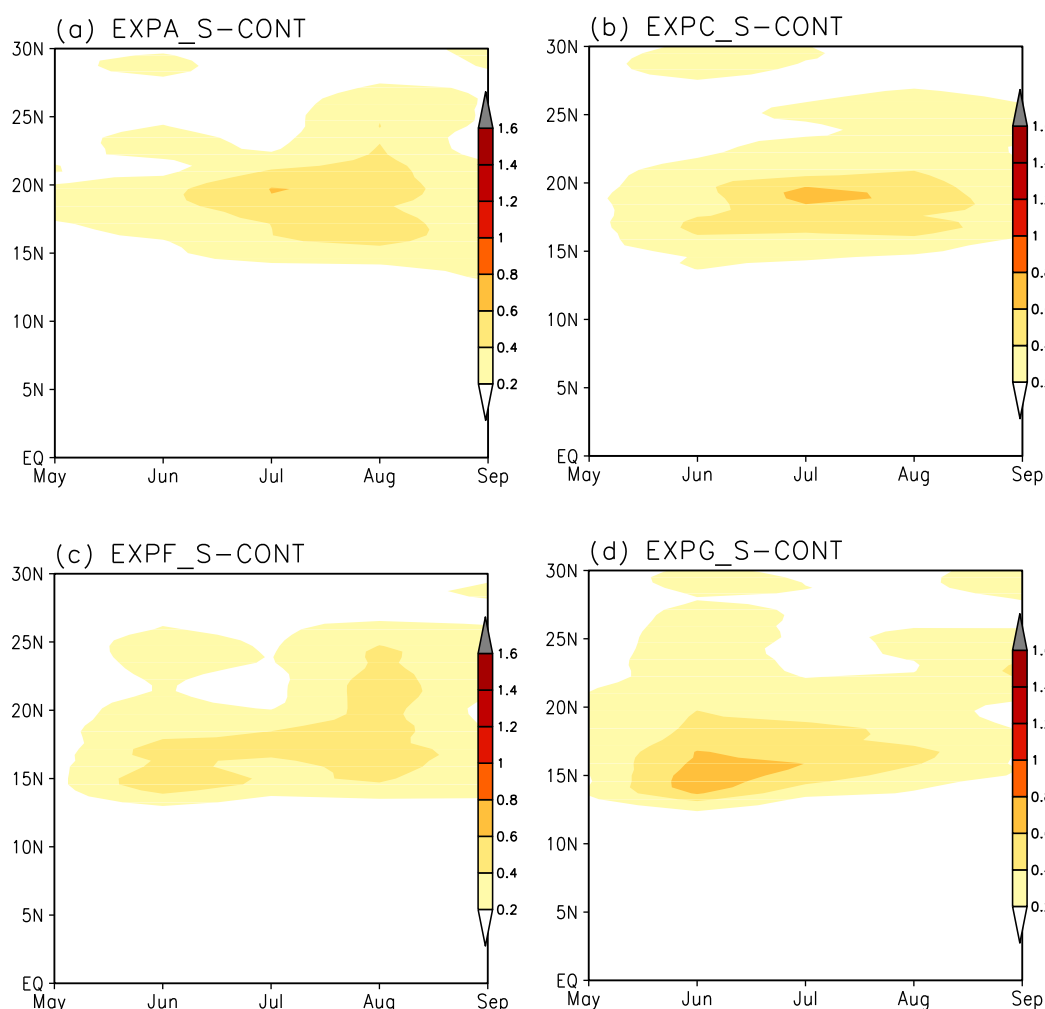


**Figure 13.** As in Figure 12 but for wind magnitude.

would collect the potentially enhanced runoff and deliver it back to the site where the water is drawn for irrigation. At the limit, such process would result in minimal impact on the river flow downstream due to water withdrawal for irrigation.

In this section, our analysis focuses on the rainfall and runoff upstream in order to assess how much water can be collected and delivered back by the river under the different irrigation scenarios defined in terms of location and scheduling. Table 2 provides the changes of accumulated rainfall and runoff volume over the upstream sub-basin relative to the amount of irrigation water applied in each of the experiments considered in this study. Adding irrigation water would moisten the soil and enhance runoff in the irrigated area itself. Therefore, by not including the irrigated area itself in the calculation of the changes in runoff, we only consider how the introduction of irrigation scheme influences the changes in runoff through changes in the circulation and rainfall distribution. Note that systematic bias in the underlying model (e.g., overestimation of runoff upstream shown as Figure 3) can be partly cancelled when taking the difference between CONT and sensitivity experiments with irrigation, even though such a model bias could affect the magnitude of response.

For the experiments without scheduling, it is found that irrigation does not result in generation of significant runoff from the upstream subbasin relative to the large amount of irrigation water. On the other hand, in EXPA\_S and EXPC\_S irrigation from the Niger River around latitude 18°N, induces significant increase in rainfall of order 150–100% in the upstream sources of the Niger River and results in significant increase in runoff accordingly. This additional runoff can be collected by the river network and delivered back toward the irrigation area.

**Table 2.** Change in Percent (%) of Accumulated Rainfall and Runoff Volume Over the Upstream Subbasin of the Niger River Relative to the Amount of Applied Water for Each Irrigation Sensitivity Experiment During MJJAS

	EXPA	EXPB	EXPC	EXPD	EXPE	EXPF	EXPG
Rainfall	26	39	41	10	−7	−17	−28
Runoff	14	19	21	1	8	3	−4
	EXPA_S	EXPB_S	EXPC_S	EXPD_S	EXPE_S	EXPF_S	EXPG_S
Rainfall	149	63	100	1	−45	−56	−59
Runoff	115	30	45	−9	−17	−21	−13

While it is true that EXPA\_S maximizes the irrigation benefit in terms of volume of water returned by the river, it is also true that the location of the irrigated area in this experiment is further north from the Niger river. In order to irrigate this area, water has to be pumped from the river and conveyed upward through a relatively long distance of a few hundreds of kilometers to the irrigation area. In this regard, EXPC\_S is considered the optimal example: although the enhancement of rainfall and runoff upstream is relatively less in EXPC\_S than EXPA\_S, delivering the water from the Niger River to the irrigation location is more feasible in EXPC\_S than EXPA\_S.

In the CONT experiment, the Inland Delta of the Niger river is not represented. However, in EXPG and EXPG\_S the region of the Inland Delta is assumed irrigated. The amount of water used to irrigate this area in the two experiments is 49 and 21 cubic kilometers, respectively. These amounts are comparable to the estimated losses of water from this Inland Delta due to evaporation. Here instead of comparing EXPA\_S and EXPC\_S to the CONT experiment, we compare them to EXPG\_S. Figures 14 and 15 present the spatial distribution of MJJAS mean rainfall and runoff difference between (each of EXPA\_S and EXPC\_S) and EXPG\_S. The spatial patterns show significant regional variability, however the simulation indicates consistent enhancement of rainfall and runoff covering large areas over the upstream subbasin, in EXPA\_S and EXPC\_S relative to EXPG\_S.

If we hypothetically assume that irrigation in area A or area C is accompanied by draining of the swamps in area G, then the differences presented in Figures 14 and 15 can be given a different interpretation. These differences would then represent the enhancement in rainfall and runoff that would result from draining area G and irrigating area A or area C. These differences are indeed more significant in size and more

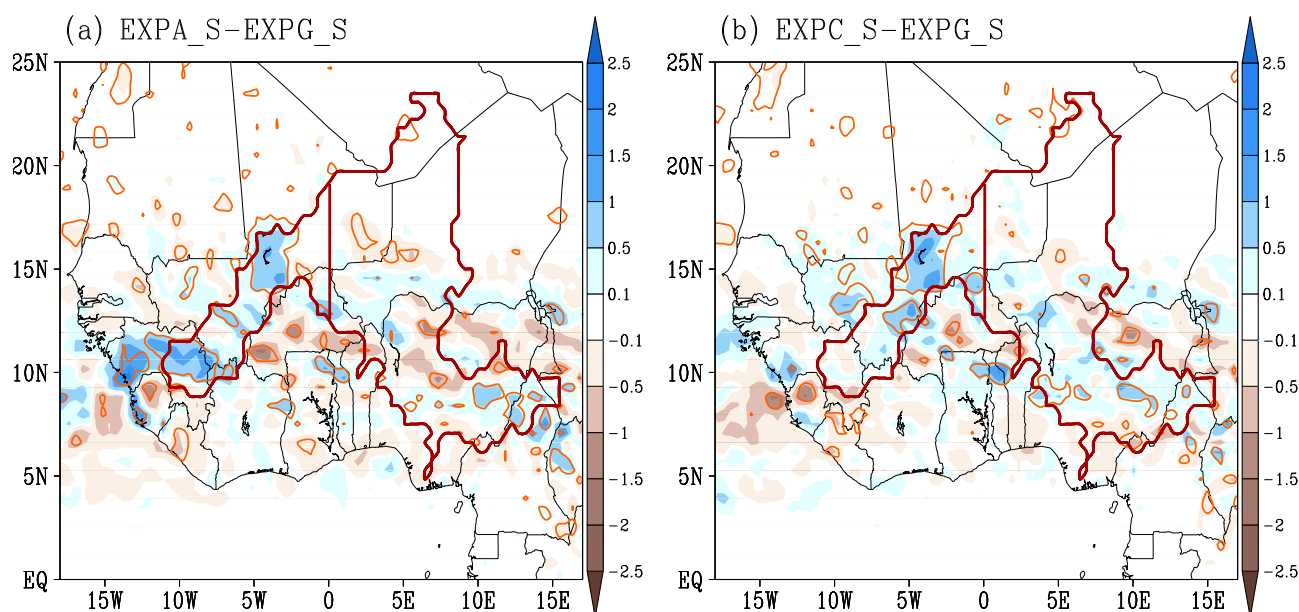


**Figure 14.** Spatial distribution of rainfall difference between EXPA\_S and EXPC\_S and EXPG\_S averaged over May to September (Unit: mm/d). Here the red outline in each plot indicates the Niger River basin and its upstream subbasin (west of 0°) used for area-averaged analysis. Areas enclosed by orange color line indicate the areas where the rainfall difference is statistically significant at the 90% confidence level.

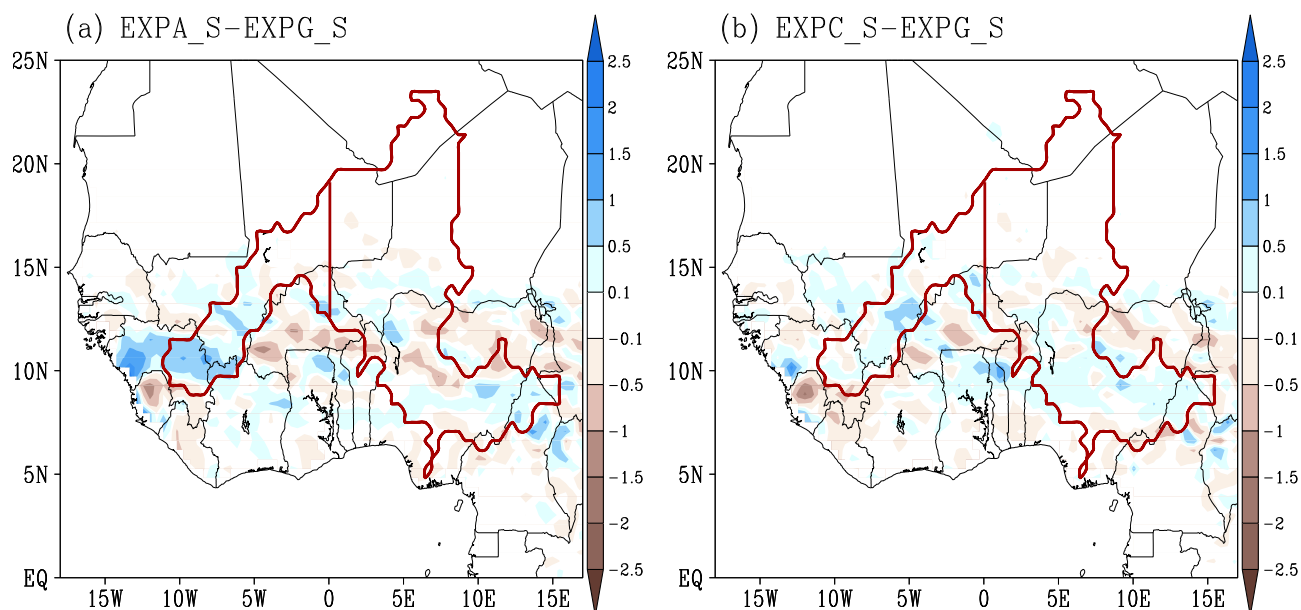


**Figure 15.** Spatial distribution of runoff difference between EXPA\_S and EXPC\_S and EXPG\_S averaged over May to September (Unit: mm/d). The irrigated area itself is not included. Here the red outline in each plot indicates the Niger River basin and its upstream subbasin (west of 0°) used for area-averaged analysis.

extensive in spatial coverage. The results of this study suggest that irrigation north of the Niger River basin (EXPA\_S and EXPC\_S) combined with draining of the swamps of the Inland Delta can improve the level of water availability significantly in this region. We regard this conclusion as preliminary and we plan to pursue future studies using different models to address this hypothesis further. The swamps of the Niger inner delta are of economic and ecological significance. In practical planning of future irrigation in the region those two sets of factors should be taken seriously. We are not proposing any specific drastic changes without consideration for the ecology.

## 5. Summary and Discussion

Although irrigation has the potential to improve agriculture productivity in West Africa, irrigation does not currently play a significant role, accounting for a small fraction of the total cultivated area [You *et al.*, 2010; KfW Development Bank, 2010]. Given that most of the area that can easily be used for agriculture is already being utilized for rain-fed agriculture [Descroix *et al.*, 2009], efforts to improve our understanding the potential for introducing and expanding irrigation are critically needed. In this study, we propose a new hypothesis describing how medium-scale irrigation (e.g., 60,000 km<sup>2</sup>) around the Niger River basin of West Africa may impact the climate conditions including the distribution of rainfall. The methodology that we followed to test our hypothesis utilizes regional climate modeling including a new representation of irrigation [Marcella, 2012; Marcella and Eltahir, 2014]. In particular, we focus on how irrigation may impact the patterns of rainfall and runoff generation upstream from the irrigation area.

In our earlier paper (Im14), we identified the mechanisms of local and remote impacts of potential large-scale irrigation (~400,000 km<sup>2</sup>) on rainfall over West Africa. Changes in rainfall are simulated not only in and around the irrigated grid cells but also across the Sahel and Gulf of Guinea far from the irrigated area. The local effect induced by strong surface cooling tends to decrease the rainfall over the irrigated area and this response is consistent irrespective of irrigation location. On the other hand, remote changes in rainfall show a significant dependence on location of irrigated area, being more sensitive to the latitudinal position rather than the longitudinal position of irrigation. The local rainfall decrease over the irrigated area induces anomalous descending motion, which associates with anticyclonic circulation that triggers the remote response. Anomalous flows derived from low-level anticyclonic circulation converge with prevailing monsoon flow at low levels. During this process, the proper timing and latitudinal position of anomalous flows can determine the strength and patterns of convergence and resultant changes in rainfall.

Large-scale irrigation experiments of Im14 clearly demonstrate the mechanisms responsible for rainfall change and suggest the optimal location of irrigated area located between latitudes of 18°N and 22°N. In the medium-scale irrigation experiments designed in this study, the size of irrigated area and the corresponding irrigation water are significantly reduced. However, the resulting responses of the climate of West Africa to irrigation are very similar with those from large-scale irrigation experiments. If the irrigated location is placed north of 17°N, the changes in rainfall and related dynamics have virtually the same structure as EXP4 of Im14, which was characterized by a significant increase in rainfall. Based on the climatological wind field, a sharp gradient in the magnitude of low-level wind occurs around 17°N–18°N in July and August. Therefore, if irrigation is located at 17°N–18°N, anomalous low-level outflows associated with the anticyclonic circulation centered at the irrigation area are placed at the optimal position to effectively converge with the background monsoon flow. Another important factor is how much irrigation water is applied. If the irrigated area is located in the relatively wet southern region, the additional amount of water needed to almost saturate the soil through irrigation would be relatively small. The relatively muted cooling associated with limited irrigation in these southern regions makes it difficult to induce strong anomalous flows during peak timing of WAM.

Another important conclusion from the experiments conducted in this study is that irrigation scheduling is a very effective tool to enhance the ratio of the gain of water in rainfall and runoff compared to the water used in irrigation. As scheduling is imposed, supplied water for irrigation is reduced to less than one-third compared to the corresponding experiment without scheduling. Nevertheless, the changes in rainfall distribution due to irrigation are indeed comparable between the two experiments. Hence, the additional water used in irrigation without scheduling does not necessarily result in a proportional response in rainfall distribution.

Finally, EXPA\_S and EXPC\_S, which are located above 17°N with scheduling, are associated with enhanced rainfall and runoff in the upstream subbasin of the Niger River. Considering the location of the irrigation area C relative to the Niger River, the irrigated area of EXPC\_S appears to be more feasible than EXPA\_S for practical application. In fact, this result requires a rethinking of the conventional view of irrigation in this region. We suggest that irrigation to the north of the Niger River basin should be looked at more favorably than irrigation around the Inland Delta. Recall that water resources of the Inland Delta are unevenly distributed, which makes water management and effective utilization difficult [You *et al.*, 2010]. By selecting the location of irrigation carefully, the positive impacts of irrigation on rainfall distribution can be maximized. The approach used in this study may be the first step in incorporating land-atmosphere interactions in the design of the location and size of irrigation projects.

The results of this study suggest that irrigation north of the Niger River basin (EXPA\_S and EXPC\_S) combined with draining of the swamps of the Inland Delta can improve the level of water availability significantly in this region. We regard this conclusion as preliminary and we plan to pursue future studies using different models to address this hypothesis further. Although the mechanism responsible for the changes in rainfall in response to irrigation in our model is well understood and has been identified in many of our experiments, the estimates of the magnitude of the changes in rainfall are somewhat uncertain and need to be further refined in future studies. In this regard, we are planning to perform two types of ensemble experiments (e.g., different initial conditions and different regional climate models). One source of uncertainty is internal variability which can be quantified using experiments with perturbed initial conditions within the same modeling system [Vanyve *et al.*, 2008]. Whether the spread of ensemble members with different initial conditions converges or diverges can determine the confidence level of response due to external forcing (e.g., irrigation). In addition, we will particularly seek to conduct studies using models that are significantly different from MRCM to confirm that our results are general, independent of the details of our model.

#### Acknowledgments

The authors acknowledge the comments by the Editor, Associate Editor, and three anonymous reviewers and their feedback and suggestions in the review process. The authors are also grateful to all members of the Eltahir group that contributed in some way to this work. This research was supported by the National Research Foundation Singapore through the Singapore MIT Alliance for Research and Technology's Center for Environmental Sensing and Modeling interdisciplinary research program.

#### References

- Abiodun, B. J., Z. D. Adeyewa, P. G. Oguntunde, A. T. Salami, and V. O. Ajayi (2012), Modeling the impact of reforestation on future climate in West Africa, *Theor. Appl. Climatol.*, **110**, 77–96.
- Ackerley, D., B. B. Booth, S. H. E. Knight, E. J. Highwood, D. J. Frame, M. R. Allen, and D. P. Rowell (2011), Sensitivity of twentieth-century Sahel rainfall to sulfate aerosol and CO<sub>2</sub> forcing, *J. Clim.*, **24**, 4999–5014.
- Andersen, I., O. Dione, M. Jarosewich-Holder, and J.-C. Olivry (2005), The Niger River Basin: A vision of sustainable management, in *Directions in Development*, edited by K. G. Golitzen, 145 pp., World Bank, Washington, D. C.
- Bader, J., and M. Latif (2003), The impact of decadal-scale Indian Ocean sea surface temperature anomalies on Sahelian rainfall and the North Atlantic Oscillation, *Geophys. Res. Lett.*, **30**(22), 2169, doi:10.1029/2003GL018426.
- Cappelaere, B., *et al.* (2009), The AMMA-CATCH experiment in the cultivated Sahelian area of south-west Niger—Investigating water cycle response to a fluctuating climate and changing environment, *J. Hydrol.*, **375**, 34–51.



- Cook, B. I., M. J. Puma, and N. Y. Krakauer (2011), Irrigation induced surface cooling in the context of modern and increased greenhouse gas forcing, *Clim. Dyn.*, **37**, 1587–1600.
- Dadson, S. J., I. Ashpole, P. Harris, H. N. Davies, D. B. Clark, E. Blyth, and C. M. Taylor (2010), Wetland inundation dynamics in a model of land surface climate: Evaluation in the Niger inland delta region, *J. Geophys. Res.*, **115**, D23114, doi:10.1029/2010JD014474.
- DeAngelis, A., F. Dominguez, Y. Fan, A. Robock, M. D. Kustu, and D. Robinson (2010), Evidence of enhanced precipitation due to irrigation over the Great Plains of the United States, *Geophys. Res. Lett.*, **115**, D15115, doi:10.1029/2010JD013892.
- Descroix, L., et al. (2009), Spatio-temporal variability of hydrological regimes around the boundaries between Sahelian and Sudanian areas of West Africa: A synthesis, *J. Hydrol.*, **375**, 90–102.
- Eltahir, E. A. B. (1998), A soil moisture-rainfall feedback mechanism. 1. Theory and observations, *Water Resour. Res.*, **34**, 765–776.
- Eltahir, E. A. B., and R. L. Bras (1996), Precipitation recycling, *Rev. Geophys.*, **34**, 367–378.
- Fekete, B. M., C. J. Vörösmarty, and W. Grabs (2002), Global composite runoff fields on observed river discharge and simulated water balances, *Tech. Rep. 22*, Global Runoff Data Cent., Fed. Inst. of Hydrol. (BfG), Koblenz, Germany.
- Fekete, B. M., C. J. Vörösmarty, J. O. Roads, and C. J. Willmott (2004), Uncertainties in precipitation and their impacts on runoff estimates, *J. Clim.*, **17**, 294–304.
- Flaounas, E., S. Bastin, and S. Janicot (2010), Regional climate modeling of the 2006 West African monsoon: Sensitivity to convection and planetary boundary layer parameterization using WRF, *Clim. Dyn.*, **36**, 1083–1105.
- Food and Agriculture Organization (FAO) (2010), AQUASTAT, Country fact sheets, United Nations, Italy. [Available at <http://www.fao.org/nr/water/aquastat/countries/index.stm>.]
- Gianotti, R. L. (2012), Regional climate modeling over the maritime continent: Convective cloud and rainfall processes, PhD dissertation, 306 pp., Mass. Inst. of Technol., Cambridge, Mass.
- Gianotti, R. L., and E. A. B. Eltahir (2014a), Regional climate modeling over the Maritime Continent. Part I: New parameterization for convective cloud fraction, *J. Clim.*, **27**, 1488–1503.
- Gianotti, R. L., and E. A. B. Eltahir (2014b), Regional climate modeling over the Maritime Continent. Part II: New parameterization for auto-conversion of convective rainfall, *J. Clim.*, **27**, 1504–1523.
- Harding, K. J., and P. K. Snyder (2012a), Modeling the atmospheric response to irrigation in the Great Plains. Part I: General impacts on precipitation and the energy budget, *J. Hydrometeorol.*, **13**, 1667–1686.
- Harding, K. J., and P. K. Snyder (2012b), Modeling the atmospheric response to irrigation in the Great Plains. Part II: The precipitation of irrigated water and changes in precipitation recycling, *J. Hydrometeorol.*, **13**, 1687–1703.
- Hernandez-Diaz, L., R. Laprise, L. Sushama, A. Martynov, K. Winger, and B. Dugas (2013), Climate simulation over CORDEX Africa domain using the fifth-generation Canadian Regional Climate Model (CRCM5), *Clim. Dyn.*, **40**, 1415–1433, doi:10.1007/s00382-012-1387-z.
- Huffman, G. J., et al. (2007), The TRMM Multisatellite Precipitation Analysis (TMPA): Quasi-global, multiyear, combined-sensor precipitation estimates at fine scales, *J. Hydrometeorol.*, **8**, 38–55.
- Im, E.-S., M. P. Marcella, and E. A. B. Elfatih (2014a), The impact of potential large-scale irrigation on the West African Monsoon and its dependence on location of irrigated area, *J. Clim.*, **27**, 994–1009.
- Im, E.-S., R. L. Gianotti, and E. A. B. Eltahir (2014b), Improving simulation of the West African monsoon using the MIT Regional Climate Model, *J. Clim.*, **27**, 2209–2229.
- KfW Development Bank (2010), *River Basin Snapshot: Adaptation to Climate Change in the Upper and Middle Niger River Basin*, Ger. Minist. of Econ. Coop. and Dev. (BMZ), Germany.
- Knoche, H. R., and H. Kunstmann (2013), Tracking atmospheric water pathways by direct evaporation tagging: A case study for West Africa, *J. Geophys. Res. Atmos.*, **118**, 12,345–12,358, doi:10.1002/2013JD019976.
- Koster, R. D., et al. (2004), Regions of strong coupling between soil moisture and precipitation, *Science*, **305**, 1138–1140.
- Kueppers, L. M., M. A. Snyder, and L. C. Sloan (2007), Irrigation cooling effect: Regional climate forcing by land-use change, *Geophys. Res. Lett.*, **34**, L03703, doi:10.1029/2006GL028679.
- Lebel, T., and A. Ali (2009), Recent trends in the Central and Western Sahel rainfall regime (1990–2007), *J. Hydrol.*, **375**, 52–64.
- Lebel, T., et al. (2009), AMMA-CATCH studies in the Sahelian region of West-Africa. An overview, *J. Hydrol.*, **375**, 3–13.
- Li, K. Y., M. T. Coe, N. Ramankutty, and R. De Jong (2007), Modeling the hydrological impact of land-use change in West Africa, *J. Hydrol.*, **337**, 258–268.
- Lo, M.-H., and J. S. Famiglietti (2013), Irrigation in California's Central Valley strengthens the southwestern U.S. water cycle, *Geophys. Res. Lett.*, **40**, 301–306, doi:10.1002/GRL.50108.
- Mahe, G., J.-E. Paturel, E. Servat, D. Conway, and A. Dezetter (2005), The impact of land use change on soil water holding capacity and river flow modelling in the Nakambe River, Burinka-Faso, *J. Hydrol.*, **300**, 33–43.
- Marcella, M., and E. A. B. Eltahir (2014), Introducing an irrigation scheme to a regional climate model: A case study over West Africa, *J. Clim.*, **27**, 5708–5723.
- Marcella, M. P. (2012), Biosphere-atmosphere interactions over semi-arid regions: Modeling the role of mineral aerosols and irrigation in the regional climate system, PhD dissertation, 282 pp., Mass. Inst. of Technol., Cambridge, Mass.
- Mitchell, T. D., T. R. Carter, P. D. Jones, M. Hulme, and M. New (2004), A comprehensive set of high-resolution grids of monthly climate for Europe and the globe: The observed record (1901–2000) and 16 scenarios (2001–2100), *Working Pap. 55*, Tyndall Cent. for Clim. Change Res., Norwich, U. K.
- Nicholson, S. E., B. Some, and B. Kone (2000), An analysis of recent rainfall conditions in West Africa, indicating the rainy seasons of the 1997 El Nino and the 1998 La Nina years, *J. Clim.*, **13**, 2628–2640.
- Nikulin, G., et al. (2012), Precipitation climatology in an ensemble of CORDEX-Africa regional climate simulations, *J. Clim.*, **25**, 6057–6078.
- Ozdogan, M., M. Rodell, H. K. Beaudoin, and D. L. Toll (2010), Simulating the effects of irrigation over the United States in a land surface model based on satellite-derived agricultural data, *J. Hydrometeorol.*, **11**, 171–184.
- Pal, J. S., et al. (2007), The ICTP RegCM3 and RegCNET: Regional climate modeling for the developing world, *Bull. Am. Meteorol. Soc.*, **88**, 1395–1409.
- Puma, M. J., and B. I. Cook (2010), Effects of irrigation on global climate during the 20th century, *J. Geophys. Res.*, **115**, D16120, doi:10.1029/2010JD014122.
- Scanlon, B. R., I. Jolly, M. Sophocleous, and L. Zhang (2007), Global impacts of conversions from natural to agricultural ecosystems on water resources: Quantity versus quality, *Water Resour. Res.*, **43**, W03437, doi:10.1029/2006WR005486.
- Segal, M., Z. Pan, R. W. Turner, and E. S. Takle (1998), On the potential impact of irrigated areas in North America on summer rainfall caused by large-scale system, *J. Appl. Meteorol.*, **37**, 325–331.

- Sorooshian, S., J. Li, K. Hus, and X. Gao (2011), How significant is the impact of irrigation on the local hydroclimate in California's Central Valley? Comparison of model results with ground and remote-sensing data, *J. Geophys. Res.*, **116**, D06102, doi:10.1029/2010JD014775.
- Sorooshian, S., J. Li, K. Hus, and X. Gao (2012), Influence of irrigation schemes used in regional climate models on evapotranspiration estimation: Results and comparative studies from California's Central Valley agricultural regions, *J. Geophys. Res.*, **117**, D06107, doi:10.1029/2011JD016978.
- Sylla, M. B., A. T. Gaye, J. S. Pal, G. S. Jenkins, and X. Q. Bi (2009), High resolution simulations of West African climate using regional climate model (RegCM3) with different lateral boundary conditions, *Theor. Appl. Climatol.*, **98**, 293–314.
- Sylla, M. B., E. Coppola, L. Mariotti, F. Giorgi, P. M. Ruti, A. Dell'Aquila, and X. Bi (2010a), Multiyear simulation of the African climate using a regional climate model (RegCM3) with the high resolution ERA-interim reanalysis, *Clim. Dyn.*, **35**, 231–247.
- Sylla, M. B., A. Dell'Aquila, P. M. Ruti, and F. Giorgi (2010b), Simulation of the intraseasonal and the interannual variability of rainfall over West Africa with RegCM3 during the monsoon period, *Int. J. Climatol.*, **30**, 1865–1883.
- Taylor, C. M. (2010), Feedbacks on convection from an African wetland, *Geophys. Res. Lett.*, **37**, L05406, doi:10.1029/2009GL041652.
- Uppala, S., D. Dee, S. Kobayashi, P. Berrisford, and A. Simmons (2008), Towards a climate data assimilation system: Status update of ERA-Interim, *ECMWF Newsl.*, **115**, 12–18.
- Vanvyve, E., N. Hall, C. Messenger, S. Leroux, and J.-P. van Ypersele (2008), Internal variability in a regional climate model over West Africa, *Clim. Dyn.*, **30**, 191–202.
- Winter, J. M., J. S. Pal, and E. A. B. Eltahir (2009), Coupling of integrated biosphere simulator to regional climate model version 3, *J. Clim.*, **22**, 2743–2756.
- You, L., et al. (2010), What is the irrigation potential for Africa? A combined biophysical and socioeconomic approach, *IFPRI Discuss. Pap. 00993*, Int. Food Policy Res. Inst., Washington, D. C.
- Zwarts, L., P. van Beukering, B. Kone, and E. Wymenga (2005), *The Niger, A Lifeline: Effective Water Management in the Upper Niger Basin*, RIZA, Lelystad/Wetlands Int., Mali, Netherlands.